

## **General Disclaimer**

### **One or more of the Following Statements may affect this Document**

- This document has been reproduced from the best copy furnished by the organizational source. It is being released in the interest of making available as much information as possible.
- This document may contain data, which exceeds the sheet parameters. It was furnished in this condition by the organizational source and is the best copy available.
- This document may contain tone-on-tone or color graphs, charts and/or pictures, which have been reproduced in black and white.
- This document is paginated as submitted by the original source.
- Portions of this document are not fully legible due to the historical nature of some of the material. However, it is the best reproduction available from the original submission.

(NASA-CR-169460) MODULATION TECHNIQUES  
(City Coll. of the City Univ. of New York.)  
47 p HC A03/MF A01 CSCL 17B

N83-10329

G3/32 Unclas  
38348

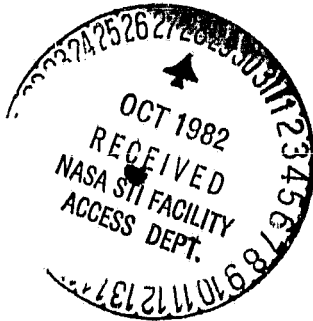
NASA-LEWIS Research Center

Cleveland, Ohio

✓ NASA Grant: NAG-3-299

Technical Report: TR - 1

MODULATION TECHNIQUES



✓ Donald L. Schilling

Professor of Electrical Engineering

Principle Investigator

COMMUNICATIONS SYSTEMS LABORATORY  
DEPARTMENT OF ELECTRICAL ENGINEERING



THE CITY COLLEGE OF  
THE CITY UNIVERSITY OF NEW YORK

NASA-LEWIS Research Center

Cleveland, Ohio

NASA Grant: NAG-3-299

Technical Report: TR - 1

MODULATION TECHNIQUES

Donald L. Schilling

Professor of Electrical Engineering

Principle Investigator

COMMUNICATIONS SYSTEMS LABORATORY

DEPARTMENT OF ELECTRICAL ENGINEERING



## TABLE OF CONTENTS

	<u>Page</u>
I. Introduction	1
II. Quadrature Phase Shift Keying	2
III. Offset- QPSK and MSK	5
IV, Combined Modulation and Coding	12
V. Spectrally Efficient Modulation Techniques	16
VI. References	40

## I. Introduction

The ever increasing demand for frequency allocation, the recent trend in employing digital methods for highly reliable communications, the bandwidth expansion of the signal by non-linear satellite channels specifically at high frequency ranges, and above all, the limited natural resource of frequency spectrum have stimulated the research and development of reliable, bandwidth efficient and high data rate communications systems. The performance of a system is evaluated according to several criteria, such as bit error rate in additive white Gaussian noise (AWGN), bandwidth allocation, signalling speed, complexity and the effects of fading, nonlinearities and interference. In a communication system the employment of many schemes such as bit rate reduction (bandwidth compression) techniques, error control methods and modulation techniques contribute to the overall performance of the system.

In this report, bandwidth efficient digital modulation techniques which have been proposed for use on and/or applied to satellite channels are briefly reviewed. In a survey of recent works on digital modulation techniques, [1], the performance of several schemes operating in various environments are compared and an extensive number of references is presented.

## II. Quadrature Phase Shift Keying

Quadrature phase shift keying (QPSK), also called 4-PSK is a well known modulation technique and is widely used in digital terrestrial and satellite systems. The structure of QPSK, or some modified version of it, is used in the implementation of the more complicated modulation techniques: QPSK, MSK, QPR, 16-PSK and QASK which are described in the following sections. Therefore, it is essential to at first understand the principle of operation of this fundamental modulation technique.

Figure 1 shows the block diagram of a QPSK modulator. The first step in generating QPSK is to separate the binary information or data sequence  $d(k)$ , where  $d(k) = \pm 1$  for  $-\infty \leq k \leq \infty$ , into two streams  $d_I(2k+1)$  and  $d_Q(2k+1)$  known as the inphase sequence and quadrature sequence, respectively. The odd bits, or the inphase sequence, are delayed by the time of one bit,  $T$ , and both the inphase sequence and quadrature sequence are stretched such that each has a duration of  $2T$ . The stretched inphase sequence and quadrature sequence are denoted by  $d_I(t)$  and  $d_Q(t)$  respectively. Note that the rate of  $d_I(t)$  and  $d_Q(t)$  is one half the rate of the original bit stream,  $d(k)$ . Next  $d_I(t)$  is amplitude modulated into a carrier  $\cos \omega_0 t$  and  $d_Q(t)$  is amplitude modulated onto the carrier  $\sin \omega_0 t$ . The two resulting terms when added together constitute the QPSK signal,  $y_{\text{QPSK}}(t)$ ,

$$y_{\text{QPSK}}(t) = d_I(t) \cos \omega_0 t + d_Q(t) \sin \omega_0 t \quad (1)$$

The signal waveforms of a specific QPSK modulated information sequence are illustrated in Fig. 2. Note that the waveform in the I and Q channel are time aligned.

Since  $d_I(t)$  and  $d_Q(t)$  are binary signals,  $y_{\text{QPSK}}(t)$  can assume four different values (phases). The signal space of a QPSK modulator with unit energy per symbol is shown in Fig. 3. The baseband signals in the I and Q channels are independent of each other. Hence the phase shift of the next transmitted signal with respect to the present signal can be 0,  $\pm 90$  or 180 degrees. The 180 degrees phase shift occurs when both components, I and Q, change their polarity. If only one of the channels changes its state, then the quadriphase signal undergoes a  $\pm 90$  degrees phase shift. Finally if both of the binary components remain the same, there are no changes in the phase of the signal. Note that the phase of the signal can change at most once per signalling time.

To avoid the AM/PM conversion phenomenon due to nonlinearities in a travelling-wave tube (TWT) satellite repeater, [2], the signal prior to the TWT is hard limited. Because of the possible abrupt phase shifts of 180 degrees in the QPSK signals, the hard limiter restores the frequency sidebands filtered out by the transmit filter [3]. In an offset-QPSK signal described in the next section, the abrupt phase shifts of 180 degrees do not occur and therefore it is more suitable for use on the nonlinear satellite channels.

### QPSK Demodulator

The QPSK signal can be detected by a coherent demodulator as shown in Fig. 4. At the receiver the received signal  $v(t)$ ,

$$v(t) = d_I(t) \cos(\omega_0 t + \theta) + d_Q(t) \sin(\omega_0 t + \theta)$$

where  $\theta$  is an unknown phase,  $0 \leq \theta \leq 2\pi$ ; is at first squared.

(For simplicity it is assumed that the received signal is noiseless).

The output of the squarer,  $v_1(t)$ , is

$$v_1(t) = d_I(t) d_Q(t) \sin(2\omega_0 t + 2\theta)$$

Note that the product  $d_I(t) d_Q(t) = p(t)$  is equal to +1 or -1.

The Costas loop used in the QPSK demodulator of Fig. 4 is a double branch phase estimator. The basic structure of a Costas loop is

shown in Fig. 5. The output of the loop to the input signal

$$v_1(t) = p(t) \sin(2\omega_0 t + 2\theta) \text{ is } v_0(t) = \cos(2\omega_0 t + 2\hat{\theta}), \text{ where } \hat{\theta}$$

is an estimate of the unknown input phase  $\theta$ . Note that  $v_0(t)$  is

independent of the waveform  $p(t)$ . For a detailed description of

the function and analysis of the voltage controlled oscillator (VCO)

and the loop filter  $H(s)$  employed in the Costas loop, the reader

is referred to ref. [4].

### Spectral Characteristic of QPSK Signals

The general approach to compute the power spectra of a random signal is to find the Fourier transform of its autocorrelation

function. The low pass equivalent of the power spectral density of

QPSK modulated signal with symbol rate  $T$  can then be readily shown to

be

$$S_{\text{QPSK}}(f) = 2T \left[ \frac{\sin 2\pi fT}{2\pi fT} \right]^2$$

## Performance of QPSK on AWGN Channel

Under ideal conditions, i.e., perfect orthogonal signalling and perfect synchronization in the coherent demodulator, the two binary components of a QPSK signal may be detected orthogonally. Thus, the absence of cross coupling between the binary components allows QPSK to provide a detection performance that is identical to the BPSK case. However, when the orthogonality between the two binary channels of a QPSK signal is destroyed by nonideal conditions, the resulting interchannel interference causes the detection performance to deteriorate. The offset-QPSK modulation technique reduces the degradation due to interchannel interference [5].

### III. Offset-QPSK and MSK

Offset-QPSK, (OQPSK), also known as staggered QPSK, is the same signalling format as QPSK except that the inphase and quadrature bit streams are offset in time by half of a symbol period. The block diagram of an OQPSK modulator is shown in Fig. 6. In Fig. 7 the waveforms at various stages of the modulator of Fig. 6 corresponding to a specific data input are sketched. Note that at each symbol interval only one of the channels may change its polarity and therefore the occurrence of phase shifts of 180 degrees are not possible. However, compared to QPSK signalling, the discontinuities in the signal phase occur more often.

The waveform of an OQPSK modulated signal is

$$y_{\text{OQPSK}}(t) = \begin{cases} d(2k-1) A(t-2kT) \cos 2\pi f_0 t + d(2k-2) B.[t-(2k-2)T] \sin 2\pi f_0 t & \text{for } (2k-1)T \leq t \leq 2kT \\ d(2k-1) A(t-2kT) \cos 2\pi f_0 t + d(2k) B(t-2kT) \sin 2\pi f_0 t & \text{for } 2kT \leq t \leq (2k+1)T \end{cases} \quad (2)$$

where modulator waveforms  $A(t)$  and  $B(t)$  are defined as

$$A(t) = \begin{cases} \frac{1}{\sqrt{2}} & \text{for } 0 \leq t \leq 2T \\ 0 & \text{otherwise} \end{cases} \quad (3)$$

and

$$B(t) = \begin{cases} \frac{1}{\sqrt{2}} & \text{for } -T \leq t \leq T \\ 0 & \text{otherwise} \end{cases}$$

In QPSK signalling, imperfect carrier synchronization produces interchannel interference. Because of offset alignment of the binary modulation components of OQPSK signals, the cross coupling can change state at midbit, such that the interference during the first half of the bit is cancelled by interference of opposite polarity during the second half of the bit interval. Consequently, OQPSK signalling will have a detection performance identical to BPSK when the cross coupling changes state, [5]. When the cross coupling remains constant over the entire bit interval the detection performance will be the same as for conventional QPSK communications.

## Power Spectra of OQPSK

The power spectral density of OQPSK is the same as the power spectral density of QPSK, i.e.,

$$S_{\text{OQPSK}}(f) = 2T \left[ \frac{\sin 2\pi fT}{2\pi fT} \right]^2$$

In systems with a purely linear channel, OQPSK modulation has no advantage over traditional QPSK signalling. However, by means of digital computer simulations [3], [6], and analytical methods [7] it is shown that the spectra of OQPSK with regard to suppression or restoration of its sidelobes is less affected by nonlinear satellite channels.

Minimum shift keying (MSK) is a special case of continuous phase frequency shift keying (CPFSK). In CPFSK the frequency is shifted or kept the same at every new data bit period [8], [9]. In MSK the frequency shift during each data bit interval  $T$ , exactly decreases or increases the phase by 90 degrees.

The signal waveform of an MSK signal is, [10]

$$y_{\text{MSK}}(t) = \cos \left[ 2\pi f_0 t + \frac{\pi d(k)}{2T} t + x(k) \right], \quad kT \leq t \leq (k+1)T \quad (4)$$

where  $f_0$  is the carrier frequency,  $d(k) = \pm 1$  is the transmitted data at rate  $R = \frac{1}{T}$  and  $x(k)$  is a phase constant which is valid over the  $k^{\text{th}}$  binary data interval  $kT \leq t \leq (k+1)T$ . The value of the constant  $x(k)$  in each bit interval is determined by the constraint that the phase of the signal at transition time  $t = kT$  must be continuous. Hence  $x(k)$  can be obtained from the recursive relation

$$x(k) = x(k-1) + [d(k-1) - d(k)] \frac{\pi k}{2} \quad (5)$$

The initial reference phase  $x(0)$ , can, without any loss of generality be set to zero. From (5) it can readily be shown that  $x(k)$  is equal to 0 or  $\pi$  modulo  $2\pi$ . Now define the piecewise linear phase function  $\phi(t)$  as

$$\phi(t) = x(k) + \left[ \frac{\pi d(k)}{2T} \right] t, \quad kT \leq t \leq (k+1)T \quad (6)$$

Then  $\phi(t)$  identifies the binary data stream  $d(k)$ ,  $-\infty \leq k \leq \infty$ , and forms a path through the phase trellis diagram of Fig. 8. As an example the phase path corresponding to a specific data stream is illustrated in Fig. 9. From Eqn. (6) or Fig. 8 it is clear that the phase  $\phi(t)$ , at times that are odd multiples of  $T$ , are  $\pm \pi/2$  modulo  $2\pi$  and at times that are even multiples of  $T$  are 0 or  $\pi$  modulo  $2\pi$ .

Using the property that  $x(k)$  is equal to zero or  $\pi$  modulo  $2\pi$  and some trigonometric identities, the MSK waveform of Eqn. (4) can be written as

$$y_{\text{MSK}}(t) = \cos(x(k)) \cos \frac{\pi t}{2T} \cos 2\pi f_0 t - d(k) \cos(x(k)) \sin \frac{\pi t}{2T} \sin 2\pi f_0 t \quad (7)$$

for  $kT \leq t \leq (k+1)T$

This representation of MSK can be interpreted as being composed of two quadrature data channels. The product  $\cos(x(k)) \cos \frac{\pi t}{2T} \cos 2\pi f_0 t$  specifies the inphase channel where  $\cos(x(k))$  is the data term,  $\sin \frac{\pi t}{2T}$  is the modulator pulse form and  $\cos 2\pi f_0 t$  is the carrier.

Similarly the product  $d(k) \cos(x(k)) \sin \frac{\pi t}{2T} \sin 2\pi f_0 t$  identifies the quadrature channel where  $d(k) \cos(x(k))$  is the data term,  $\sin \frac{\pi t}{2T}$  is the modulator pulse form and  $\sin 2\pi f_0 t$  is the quadrature carrier. Equation (7) when viewed as a quadrature signalling waveform can be rewritten as

$$y_{\text{MSK}}(t) = \begin{cases} d(2k-1) C(t-2kT) \cos \omega_0 t - d(2k-2) D(t-(2k-2)T) \sin \omega_0 t \\ \quad \text{for } (2k-1)T \leq t \leq 2kT \\ d(2k-1) C(t-2kT) \cos \omega_0 t - d(2k) D(t-2kT) \sin \omega_0 t \\ \quad 2kT \leq t \leq (2k+1)T \end{cases} \quad (8)$$

where  $C(t) = \cos \frac{\pi t}{2T}$  and  $D(t) = \sin \frac{\pi t}{2T}$ .

The block diagram of an MSK modulator is shown in Fig. 11. Note that the difference between the waveforms of OQPSK defined in (2) and  $y_{\text{MSK}}(t)$  (Eqn. (8)), is that there is no phase discontinuity in MSK. The modulator waveform of QPSK, OQPSK and MSK are presented in Fig. 10.

### Power Spectral Density of MSK

The power spectral density of MSK signal is, [10].

$$S_{\text{MSK}}(f) = \frac{8T[1+\cos 4\pi fT]}{\pi^2 [1-16 T^2 f^2]}$$

The width of the main lobe of the MSK spectrum is 1.5 times larger than the main lobe of OQPSK spectrum. However, the sidelobe drop-off is proportional to  $\frac{1}{fT}$  compared to only  $\frac{1}{f^2}$  for OQPSK and conventional QPSK. A discussion of appropriate filtering of the MSK signal to increase its bandwidth efficiency on linear channels is presented in [11].

### Detection of MSK Signals

The carrier waveform of an MSK signal defined in (4) can be written as

$$y_{\text{MSK}}(t) = \cos \left[ 2\pi \left( f_0 + \frac{d(k)}{4T} \right) t + x(k) \right]$$

Let  $f_1 = f_0 + \frac{1}{4T}$  and  $f_2 = f_0 - \frac{1}{4T}$ . Hence

$$y_{\text{MSK}}(t) = \begin{cases} \cos(2\pi f_1 t + x(k)) & \text{if } d(k) = 1 \\ \cos(2\pi f_2 t + x(k)) & \text{if } d(k) = -1 \end{cases}$$

Now, since  $x(k)$  is equal to 0 or  $\pi$ , the received MSK waveform is

$$y_{\text{MSK}}(t) = \begin{cases} \pm \cos 2\pi f_1 t & \text{if } d(k) = 1 \\ \pm \cos 2\pi f_2 t & \text{if } d(k) = -1 \end{cases}$$

The transmitted waveform of an MSK modulated data bit stream is shown in Fig. 9. The difference between the transmitted frequencies  $f_1$  and  $f_2$  is  $f_1 - f_2 = \frac{1}{2T}$  which is one half of the data bit rate.

The demodulator of MSK, Fig.12, consists of two main parts, [8]. The first part is the self synchronizing circuit and the second part is the coherent receiver. Carrier recovery and coherent demodulation can be accomplished by the squaring and phase locked loop operation shown in Fig. 13. The waveforms at different stages of the synchronization circuit are shown in the figure. Figure 14 is a detailed block diagram of the MSK coherent detector. The operation of the coherent detector is to find the phase path  $\phi(t)$  corresponding to the data sequence  $d(k)$ . Once the phase

path is known the data stream can be extracted from it. Note that the output of the correlators in Fig. 14 are integrated over two bit intervals.

$$I(2kT) = \int_{-T+2kT}^{T+2kT} \cos \omega_0 t \cos \frac{\pi t}{2T} r(t) dt$$

$$I((2k+1)T) = \int_{2kT}^{2T+2kT} \sin \omega_0 t \sin \frac{\pi t}{2T} r(t) dt$$

A serial MSK system has been proposed [12], [13] for implementation of MSK signal at high data rate. In a serial MSK system the MSK modulated signal is produced from biphase signal by filtering it with an appropriately designed conversion filter which, ideally, has a  $\sin x/x$  frequency response. Similar to the serial modulator, a serial demodulator is composed of a filter matched to the transmitted signal, followed by coherent demodulation.

In summary, QPSK modulation compared to OQPSK and MSK is inferior in both spectral characteristic and performance on various conditions. This is because of two reasons: 1) data sequence in the I and Q channels of the QPSK are uncorrelated, 2) the modulator pulse waveform of the QPSK has a rectangular shape. It is well known that these factors contribute to the undesired spectral characteristic of QPSK. Indeed, in OQPSK the data stream in the I and Q channels are correlated by half of a symbol interval and in MSK the employment of sinusoidal modulator pulses improves on out-of-band frequency drop-off.

Based on the MSK concept several "wave shaping", [14] - [19], and/or "correlation" [20] - [26] schemes have been proposed and

investigated. For example in tamed frequency modulation, [20], the signal phase at each signaling interval is a function of three consecutive bits in contrast to the phase of MSK signal which depends on two succeeding bits.

In quadrature overlapped raised-cosine modulation (QORC), [23], the modulator pulse shape takes form of an overlapping raised-cosine  $\frac{1}{2} (1 - \cos \frac{\pi t}{T})$ , for  $0 \leq t \leq 2T$ , which are extended over two data bit interval. The power spectral density of QORC is shown to be equivalent to the product of the power spectral densities of MSK and QPSK, i.e., the power spectral density of the main lobe retains the width of the spectral density main lobe of QPSK and the sidelobes drop-off by the order of  $\frac{1}{f^2}$ .

#### IV. Combined Modulation and Coding

In ordinary digital systems the transmitter consists of two main parts, a digital-to-digital binary encoder and a digital to-analog converter called a modulator. The distance between encoder output codewords is measured by Hamming distance and the optimum encoder is the one which maximizes the minimum Hamming distance between the codewords.

A channel is specified by its noise characteristic, bandwidth, power limits (nonlinearities), interference and signal fade. The modulator converts the binary sequence into an analog waveform which is most suitable for transmission over the channel. In an orthogonal basis, geometrically, each waveform can be represented by a point in Euclidean space. The distance between two waveforms is the Euclidean distance between their points and the reliability

is directly proportional to this distance, [27].

Recently a number of space encoded systems have been investigated, [28], [29], where coding takes place in signal space as part of the modulation process. The main advantage of this approach is the possibility of achieving performance improvement compared to uncoded modulation without bandwidth expansion. Multi-h phase codes, [28] and Ungerboeck codes, [29], are two of the most promising signal space coding techniques.

### Multi-h Phase Codes

Consider a constant envelope continuous phase signal

$$s(t) = \cos(\omega_0 t + \phi(t))$$

where  $\phi(t)$  is the information carrying phase function. In MSK signalling the function  $\phi(t)$  is a piecewise continuous path along the phase trellis of Fig. 8, and each path can be considered as a codeword in the signal space. Note that two paths stemming from a given point in this diagram can merge just after two signalling intervals. The main idea of multi-h coding is to keep the codewords far apart in phase by means of cyclically time varying the modulation index  $h$ . For example, for information bit 0, let the phase function always change linearly with slope zero, while, for information bit 1 let the phase change linearly with slope  $h_o = \frac{1}{2}$  during the odd signalling intervals and with slope  $h_e = \frac{3}{4}$  during the even signalling intervals. Here  $h_o$  and  $h_e$  are the cyclic time varying modulation indexes and the phase trellis of this code is sketched in Fig. 15.

The horizontal lines correspond to information bit 0. Since the phase is modulo  $2\pi$ , the phase trellis actually lies on a cylinder and the phase transitions around the back of the cylinder are shown by broken lines. Note that in the trellis diagram of Fig. 15 two paths merge after at least three intervals.

The coding problem in multi-h codes is how to choose the cyclically time varying modulation indexes such that the free distance of the phase codewords in the signal space is maximized. A survey of this signalling method is given in [30] and more recent works on this subject can be found in [31].

#### Ungerboeck Codes

The concept of signal space Ungerboeck codes [29] is that for a fixed information rate, at a sufficiently high signal to noise ratio, if the number of possible channel signals is increased, it is possible to achieve a significant reliability improvement, [27]. Here the main coding problem is how to encode the information into an expanded signal space so as to achieve this gain.

The coding process is best understood by an example which consists of convolutional coding followed by a nonlinear mapping of the encoder outputs onto the set of channel signals.

In QPSK modulation, with unit energy per symbol, the minimum Euclidean distance between adjacent signal points is  $\sqrt{2}$  (see Fig. 3). Now suppose that the inphase sequence  $d_I(k)$  and the quadrature sequence  $d_Q(k)$  are passed through the rate 2/3 convolutional encoder of Fig. 16. The output of the encoder consists of three bit streams

denoted by  $y_1(k)$ ,  $y_2(k)$  and  $y_3(k)$ , and this is then used to modulate an 8-PSK signal. Since the encoder consists of 3 binary memory elements the total number of possible states of the encoder is  $2^3=8$ , and for each state there are  $2^2=4$  possible successor states. This specifies the trellis diagram of Fig. 17.

The mapping from the binary three-tuples  $y_1(k)$ ,  $y_2(k)$ ,  $y_3(k)$  to a point in the signal space of an 8-PSK is chosen such that the minimum Euclidean distance between the trellis paths is maximized. This is accomplished by a process called "mapping by set partitioning", where the 8-PSK signal set is successively partitioned into subsets with increasing subset minimum distance  $d_0 < d_1 < d_2$  as shown in Fig. 18. These subsets are then assigned to the encoder outputs.

Ungerboeck has shown that this signalling assignment maximizes the free Euclidean distance between the trellis paths. The numbers shown on the trellis branches are the actual transmitted 8-PSK signals assigned by the process of Fig. 18. The free Euclidean distance of the eight-state trellis of Fig. 17 is found to be  $d_{\text{free}} = 2.141$  which corresponds to a coding gain of 3.6dB over conventional QPSK, with no bandwidth expansion.

The Ungerboeck codes are further studied in [29], [32]-[34]. Finally, in [35] the performance of multi-h codes and Ungerboeck codes over band-limited nonlinear channels are investigated and compared by means of digital computer simulations.

## V. Spectrally Efficient Modulation Techniques

In the previous sections several modulation techniques were investigated. It was mentioned that "modulator waveform" shaping and "correlation" techniques reduce the bandwidth of the main lobe of the signal. Another method to increase the bandwidth efficiency of a system, which is defined as the number of bits/sec that can be transmitted per unit of base-bandwidth, bits/sec/Hz, is to use correlative coding, [36]. In such a system, multilevel signals are used. Duobinary/partial response signals are well known multilevel signaling techniques that control the spectral properties of the signal and cope better with channel distortions. In this section multilevel modulation techniques QPR, QASK and 16-PSK with high bandwidth efficiency are studied.

### Quadrature Partial Response (QPR)

The block diagram of a QPR modulator is shown in Fig. 19. The QPR modulator can be considered as two 3-level duobinary signals in quadrature, [36]. The even (odd) data bits in the inphase (quadrature) channel is at first differentially encoded and the output stream  $a_e(k)$ . ( $a_o(k)$ ) is fed into an impulse generator. The transfer function of the filters  $H_e(f)$  and  $H_D(f)$  is

$$|H_e(f)|^2 = |H_D(f)|^2 = H(f) = \begin{cases} 2T \cos \pi f T & \text{for } |f| \leq \frac{1}{2} T \\ 0 & \text{otherwise} \end{cases} \quad (10)$$

The generated QPR signal  $y_{QPR}$  is

$$y_{QPR}(t) = b_e(t) \cos \omega_0 t + b_o(t) \sin \omega_0 t$$

where  $b_e(t)$  and  $b_o(t)$  are three level partial response signals,

$$b(t) = \sum_{k=-\infty}^{\infty} a(k) h(t-kT)$$

and where  $h(t)$  is the impulse response of the filter with transfer function  $H_e(f)$  as defined in (10).

In a QPR modulator, for a random binary input data stream with equally likely symbols nine distinct signal points are generated, with different a priori probabilities as shown in Fig. 20.

The complexity of the QPR system is comparable to the complexity of QPSK signalling while it is less complex than the implementation of 8-PSK system. The bandwidth efficiency of QPR is 4 bits/sec/Hz and with appropriate filtering a bandwidth efficiency of 4.5 has been reported, [37]. However, from a performance point of view the 3-level QPR requires about 3-dB more signal power than QPSK. (This is expected since the efficiency of QPSK is 2 bits/sec/Hz.)

The block diagram of a QPR demodulator is sketched in Fig. 21. At the receiver at first the quadrature components are separated and filtered. The remainder of the operations in each branch is equivalent to conversion of the duobinary encoded sequence to the data streams  $d_e(k)$  and  $d_o(k)$ . The output of the filters,  $v(t)$ , are sampled at the instants

$$t = (2k-1)T/2 \quad \text{for } k=1, 2, 3, \dots$$

The sample points  $v[(2k-1)T/2]$  are squared and fed to the negative input of a comparator. The comparator outputs correspond to the even and odd data bits. The probability of an error in a QPR system is

$$P(\epsilon) \leq 2 \operatorname{erfc} \sqrt{\frac{\pi^2 E_b}{16 N_0}}$$

### Quadrature Amplitude Shift Keying (QASK)

Quadrature amplitude shift keying (QASK), also known as quadrature amplitude modulation (QAM), is a bandwidth efficient, 16-level signalling method, where the data stream is amplitude and phase modulated. The 16 signal levels can be arranged in the signal space in various ways, [39]. The signal constellation of QASK illustrated in Fig. 22 has attracted particular attention because of its high transmission efficiency and ease of realization.

The modulator of a QASK signal can be readily implemented by noting that each signal point can be decomposed into the vector sum of two QPSK modulated signals with appropriate amplitude ratios and phase relationships. The QASK modulator shown in Fig. 23 is known as the "superimposed modulation" scheme and is due to Ref. [39]. The two QPSK modulated signals  $S_1(t)$  and  $S_2(t)$  are called first-path and second-path signals, respectively. The signal level in the second path is 6dB lower than the first-path signal level. The 16-level QASK signal  $y_{\text{QASK}}(t)$  is

$$y_{\text{QASK}}(t) = S_1(t) + S_2(t) = [d_{11}(k) \cos \omega_0 t + d_{12}(k) \sin \omega_0 t] \\ + \frac{1}{2} [d_{21}(k) \cos \omega_0 t + d_{22}(k) \sin \omega_0 t]$$

where  $\omega_0$  is the carrier angular frequency and  $d_{ij}(k)$  are equal to  $\pm 1$ . Note that the rate of data signals  $d_{ij}(k)$  is one-fourth of the rate of the input data signal  $d(k)$ . The superimposed modulation scheme has the advantage that highly accurate QASK modulated signals can be easily obtained, using QPSK modulators. The implementation of the superimposed modulation scheme operating at 400 Mbit, 16-level or equivalently 1.6Gb/sec. was reported in [40]. QASK operates with a bandwidth efficiency of 4 bits/sec/Hz. The probability of error of 16-QASK is

$$P(e) \leq 2 \operatorname{erfc} \sqrt{0.4 \frac{E_b}{N_0}}$$

which is significantly greater than that of QPR.

#### Demodulation of QASK Signals

Several demodulation systems for detection of QASK modulated signals are available [41]-[43]. The block diagram of a QASK demodulator assuming perfect synchronization is shown in Fig. 24. It has two quadrature channels each containing a correlator followed by a multiple threshold detector. The output of the threshold detectors is a pair of numbers  $\hat{d}_e(k)$  and  $\hat{d}_o(k)$  which represent the estimates of the quadrature components of the transmitted signal point.

In offset-QASK the quadrature components of the signal is delayed by one-half of the symbol period,  $T/2$ . A modified version of offset-QASK with sinusoidal modulator (similar to MSK waveforms) with improved spectral roll off was proposed in [44] and implemented in [45].

## 16 PSK

In 16-PSK the sixteen signal points are equally spaced around the circumference of a circle in the amplitude-phase space. Each signal point corresponds to 4 data bits and hence the spectral efficiency of the system is 4 bits/sec/Hz.

One way to generate 16-PSK signals is shown in Fig. 25. The 16 vectors required for the 16-PSK modem are derived from a carrier generator. Selection of the appropriate vector at a given signalling interval depends on the four parallel data stream inputs to the commutative device. The signal generation method of Fig. 25 can be implemented by high speed ECL devices using VLSI techniques and is flexible, i.e., it can be modified to generate phase shift keyed signals with any required spectral efficiency, [46].

The probability of error of 16-PSK,  $P_{e,16\text{-PSK}}$  in an AWGN channel with two sided spectral power  $N_0$  can be bounded by

$$P_{e,16\text{PSK}} \leq \text{erfc} \sqrt{0.15 E_b/N_0}$$

It is seen that 16-QASK outperforms 16-PSK signalling. Moreover the demodulator of 16-PSK needs to be designed with high resolution to distinguish between the signal points.

### Demodulation of M-PSK Signals

Differentially encoded 16-PSK signals can be detected by the demodulator scheme shown in Fig. [26]. In the differentially coherent receiver signal  $\sin(\omega_0 t + \phi_i)$  is multiplied by the reference carrier signal (at  $f_0$ ) which is generated by a local oscillator.

The phase difference,  $\phi(t)$ , between the reference carrier and the received carrier is assumed to be constant over a symbol interval.

$$V_{LO} = \sin (\omega_0 t + \phi(t))$$

The inphase and quadrature components of the signal are integrated over one symbol period and sampled to produce  $I_I(iT)$  and  $I_Q(iT)$ . An estimate of  $\hat{\theta}(iT) + \phi(iT)$  can be obtained by a  $\tan^{-1}$  operation. The difference between two successive estimated phases then provides  $\hat{\theta}(iT) - \hat{\theta}((i-1)T)$  which is compared to  $2\pi K/16$  modulo  $2\pi$  to find an estimate for received symbol.

The differentially coherent demodulator of Fig. 26 is rather simple to implement. However, the circuit simplification is obtained at the expense of degraded performance, [2].

## Conclusion

The performance of the different modulation techniques are summarized in Fig. 27. In this figure the ordinate is the ratio of bit rate to basebandwidth, bits/sec/Hz and the abscissa is the signal-to-noise ratio. All curves are plotted for a bit error rate of  $10^{-4}$  and compared to Shannon's limit.

Note that QAM is efficient since its slope is parallel to Shannon's limit as complexity increases. However MPSK is inefficient. On the other hand if the receiver is nonlinear there are distinct advantages in using MPSK since it is not amplitude sensitive.

ORIGINAL PAGE IS  
OF POOR QUALITY

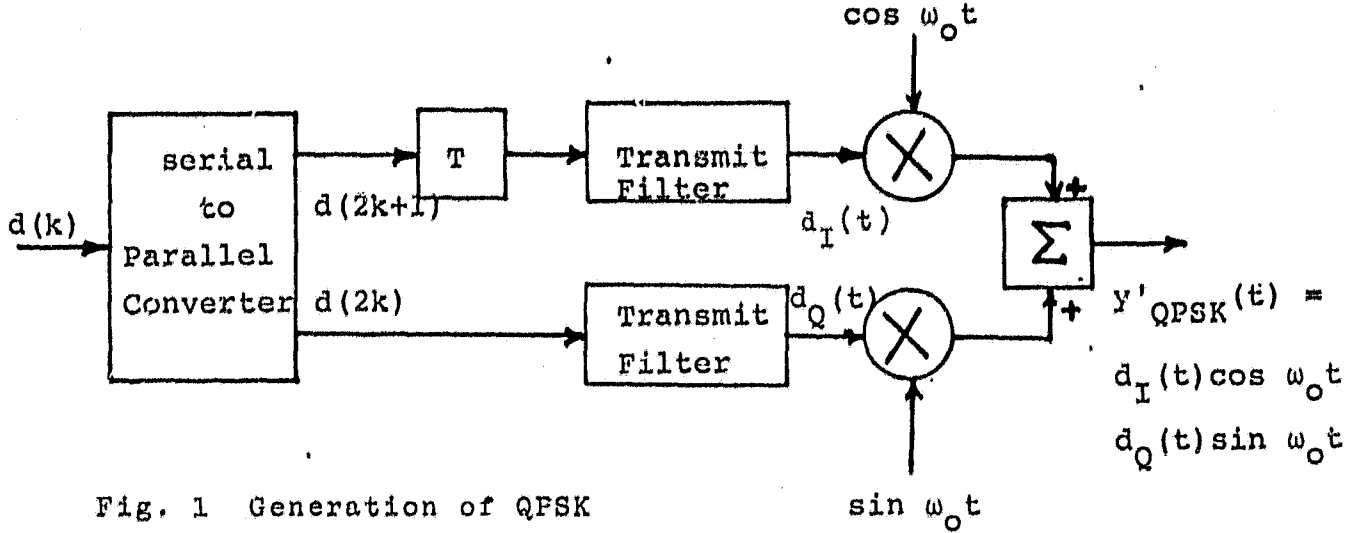


Fig. 1 Generation of QPSK

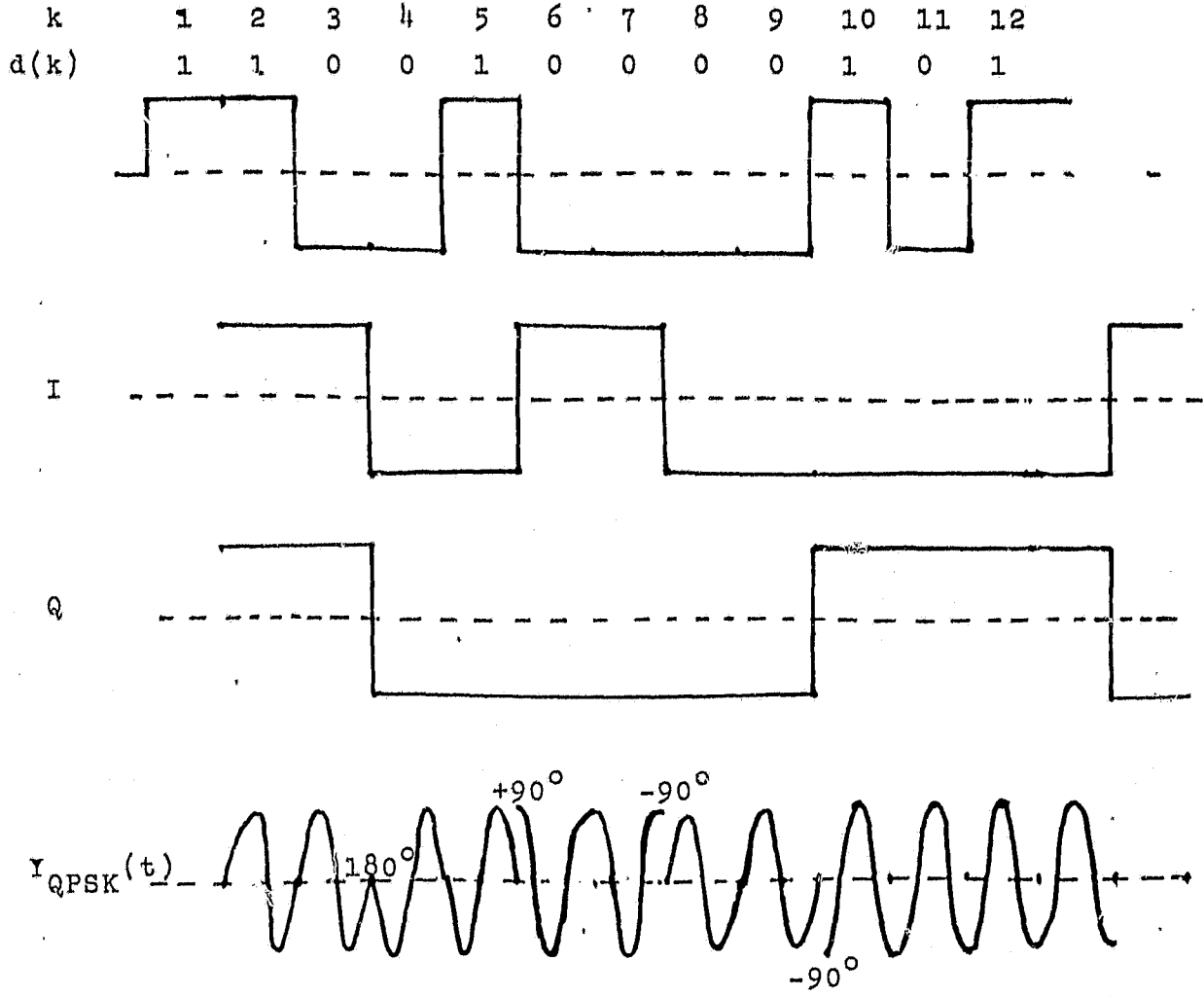


Fig. 2

ORIGINAL PAGE IS  
OF POOR QUALITY

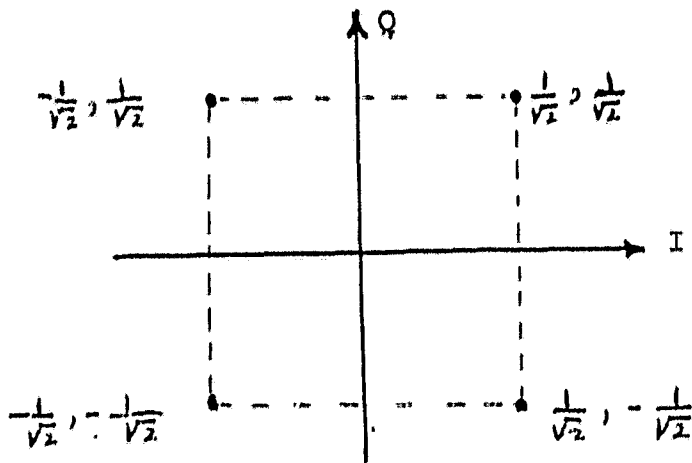


Fig. 3 Signal Space of QPSK

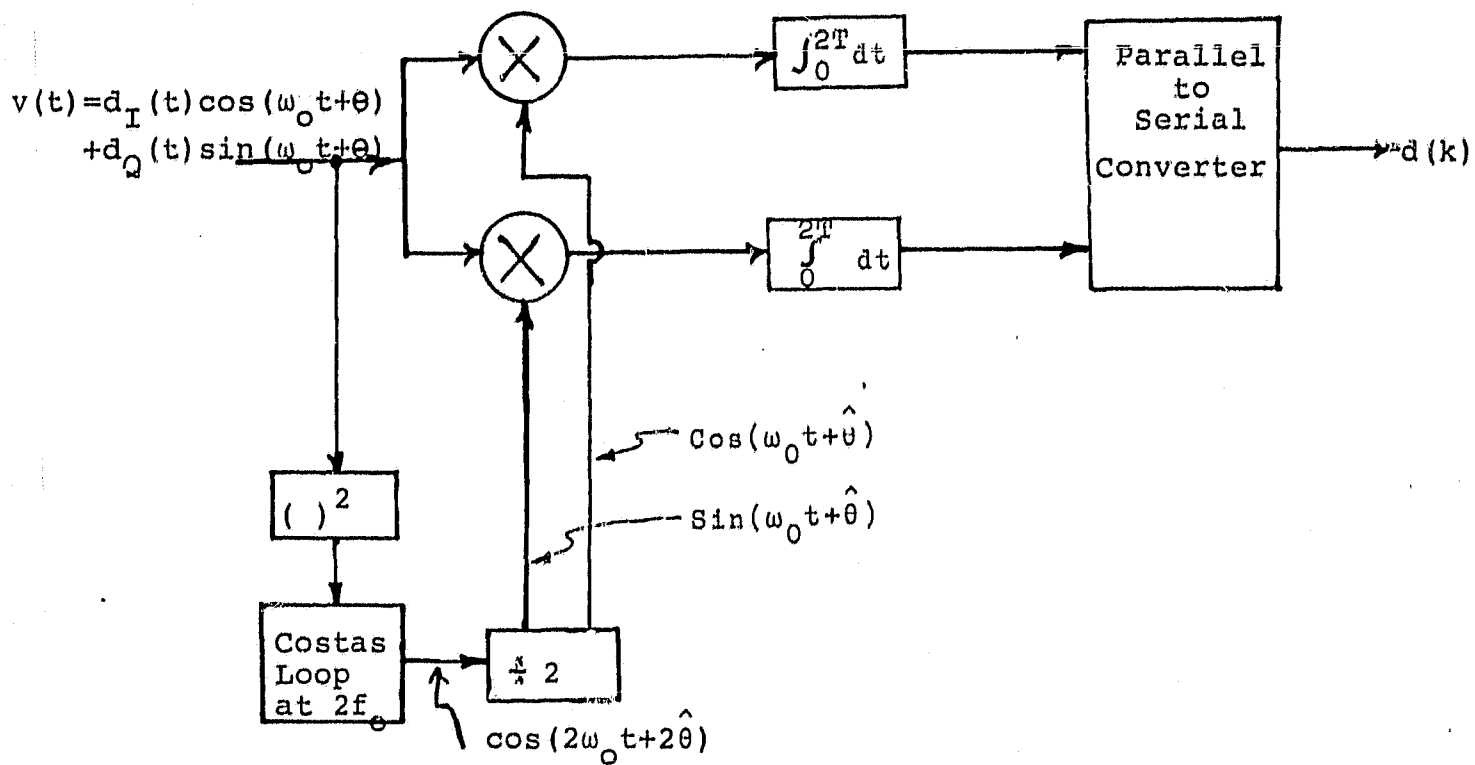


Fig. 4 QPSK Demodulator

ORIGINAL TRANSMISSION  
OF POOR QUALITY

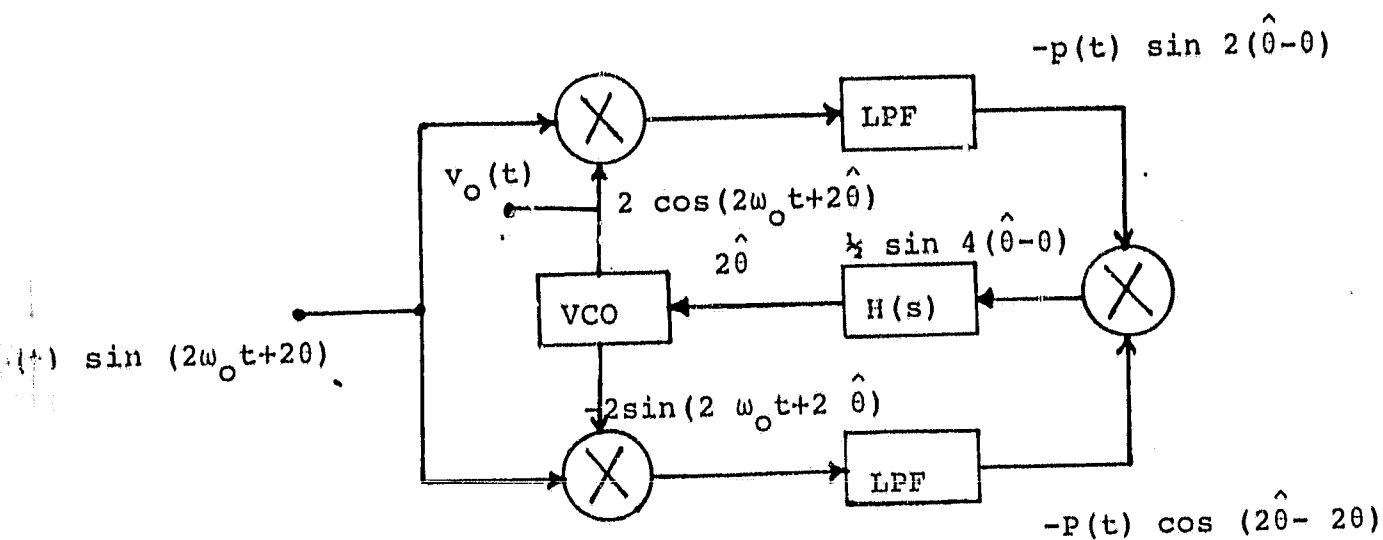


Fig. 5 Block Diagram of a Costas Loop  
set at  $2f_0$ .

ORIGINAL PAGE IS  
OF POOR QUALITY

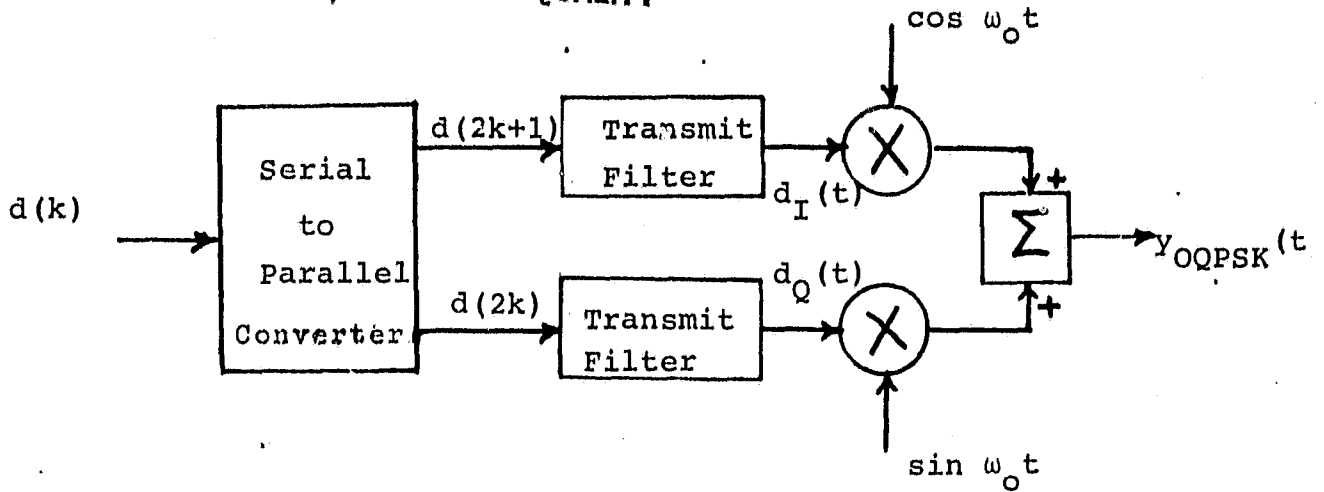


Fig. 6 Offset QPSK Modulator

k	1	2	3	4	5	6	7	8	9	10	11	12
d(k)	1	1	0	0	1	0	0	0	0	1	0	1

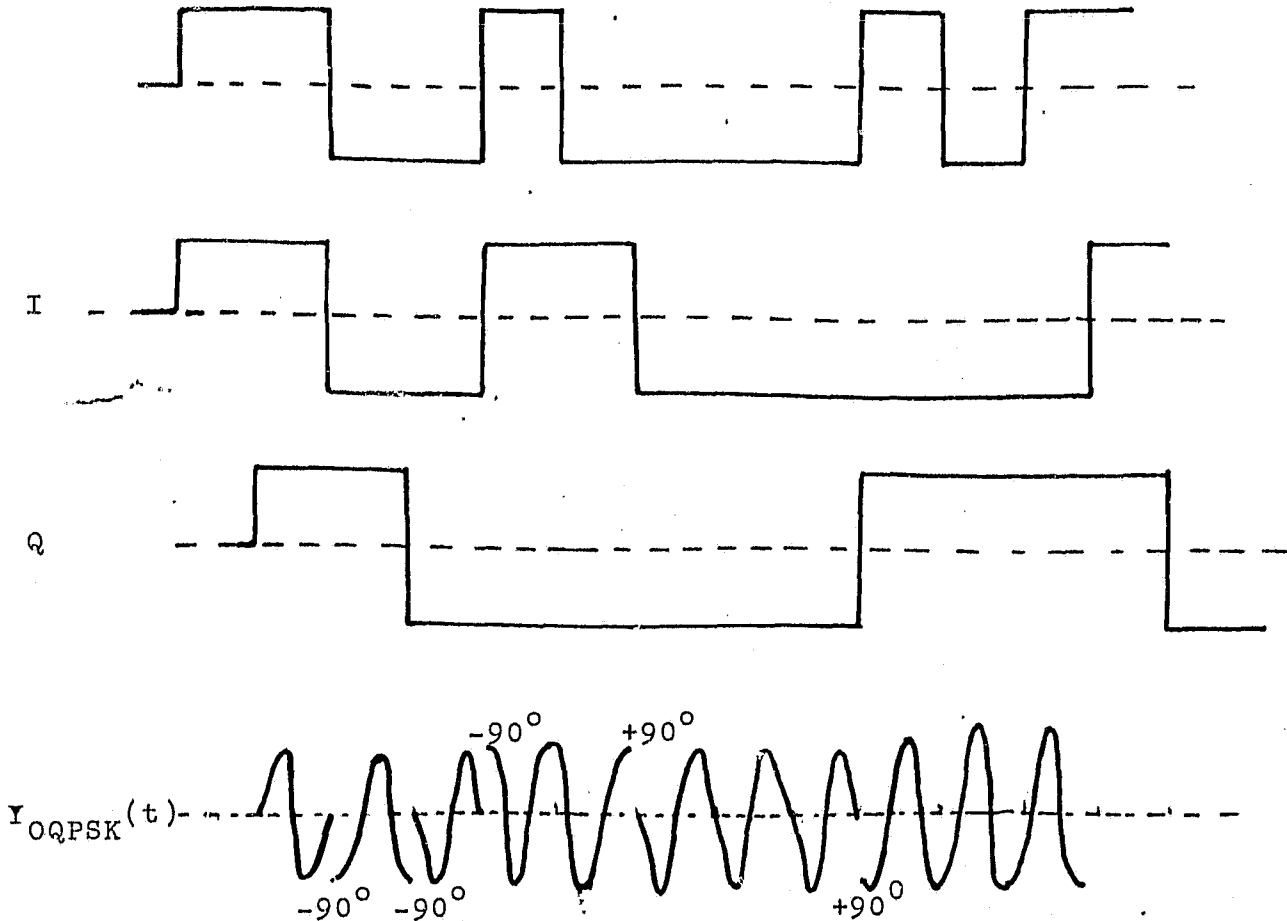


Fig. 7 OQPSK Waveforms

ORIGINAL PAGE IS  
OF POOR QUALITY

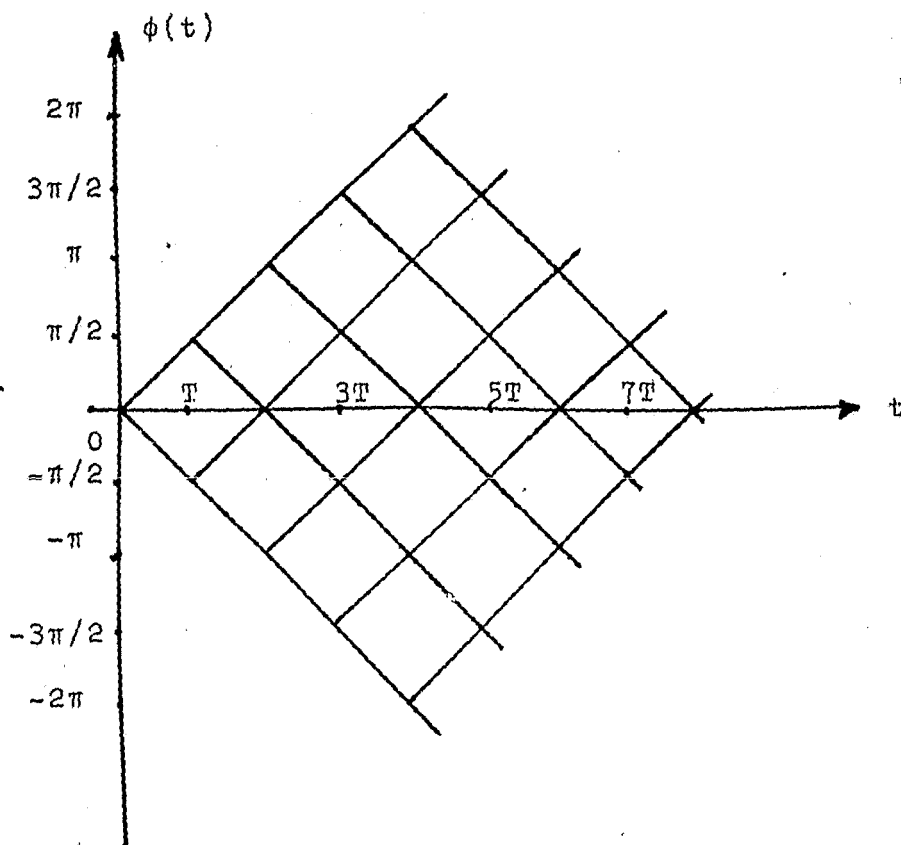


Fig. 8 MSK Phase Trellis.

ORIGINAL PAGE IS  
OF POOR QUALITY

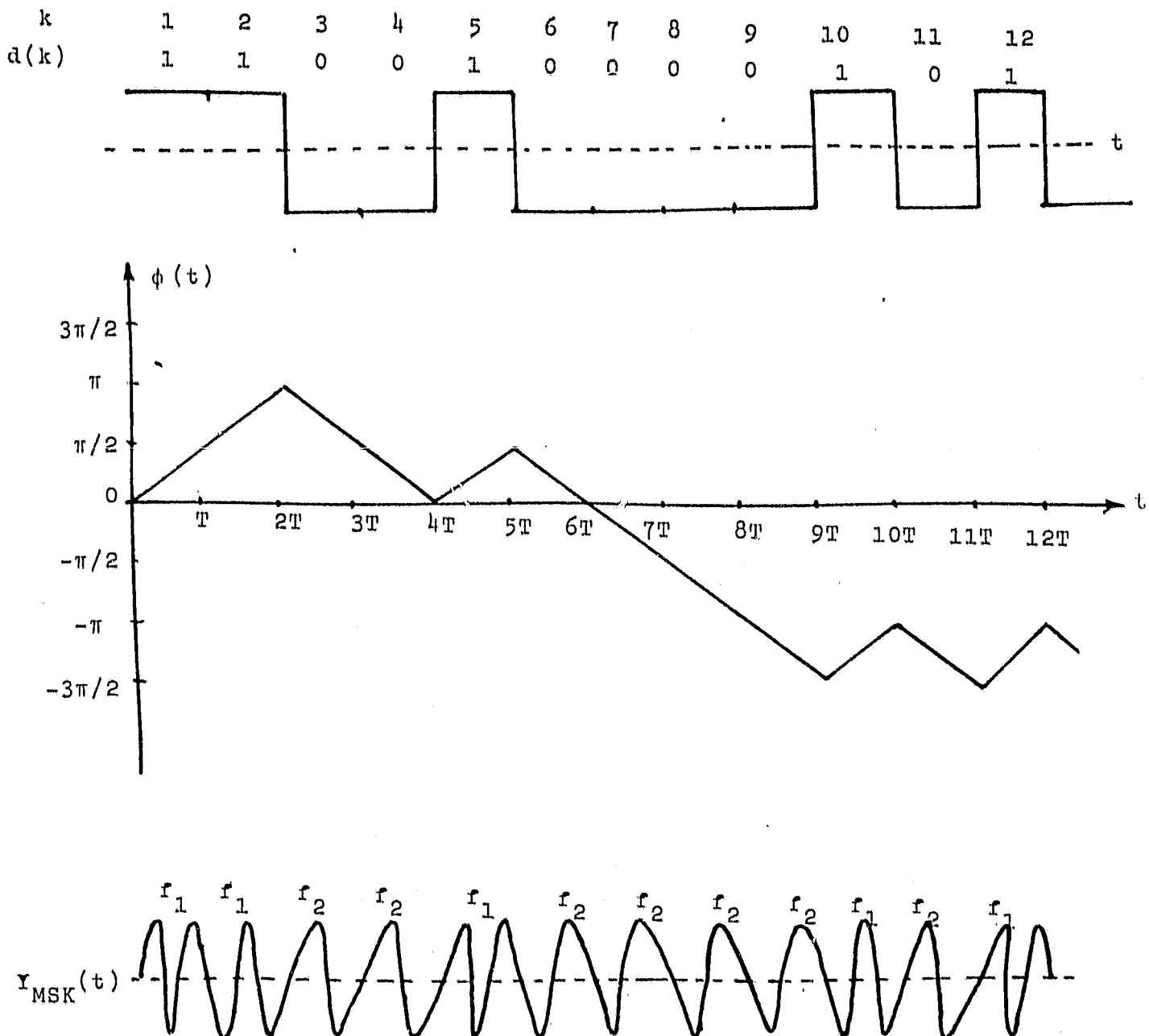


Fig. 9 Phase Waveforms of MSK Signal

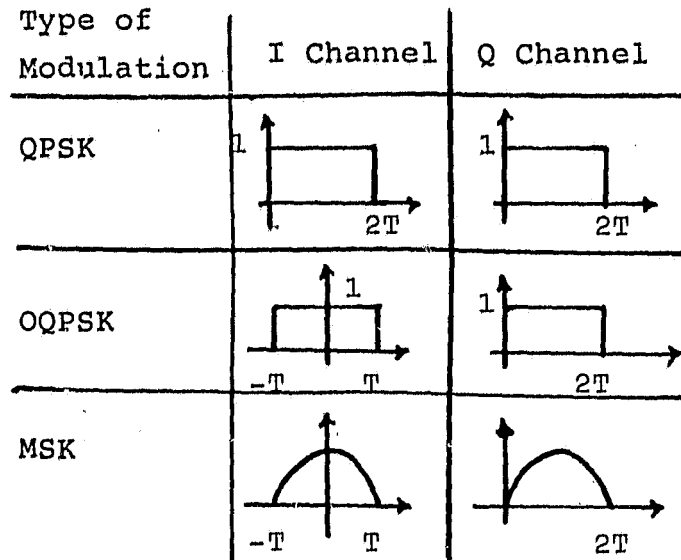


Fig. 10 Modulator Pulse Forms for Various Modulators

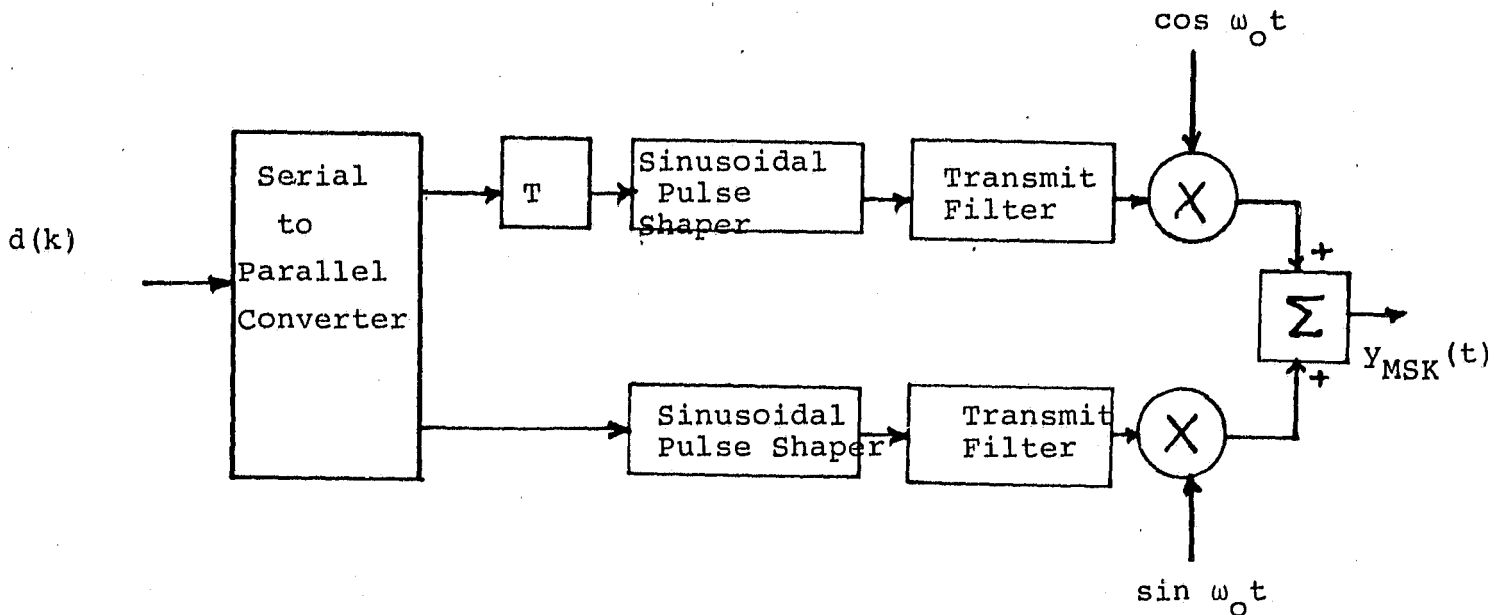


Fig. 11 MSK Modulator

ORIGINAL PAGE IS  
OF POOR QUALITY

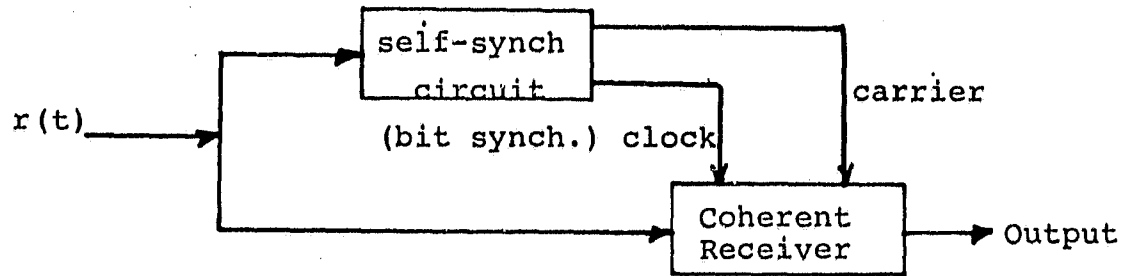


Fig. 12 Self-Synchronizing Receiver

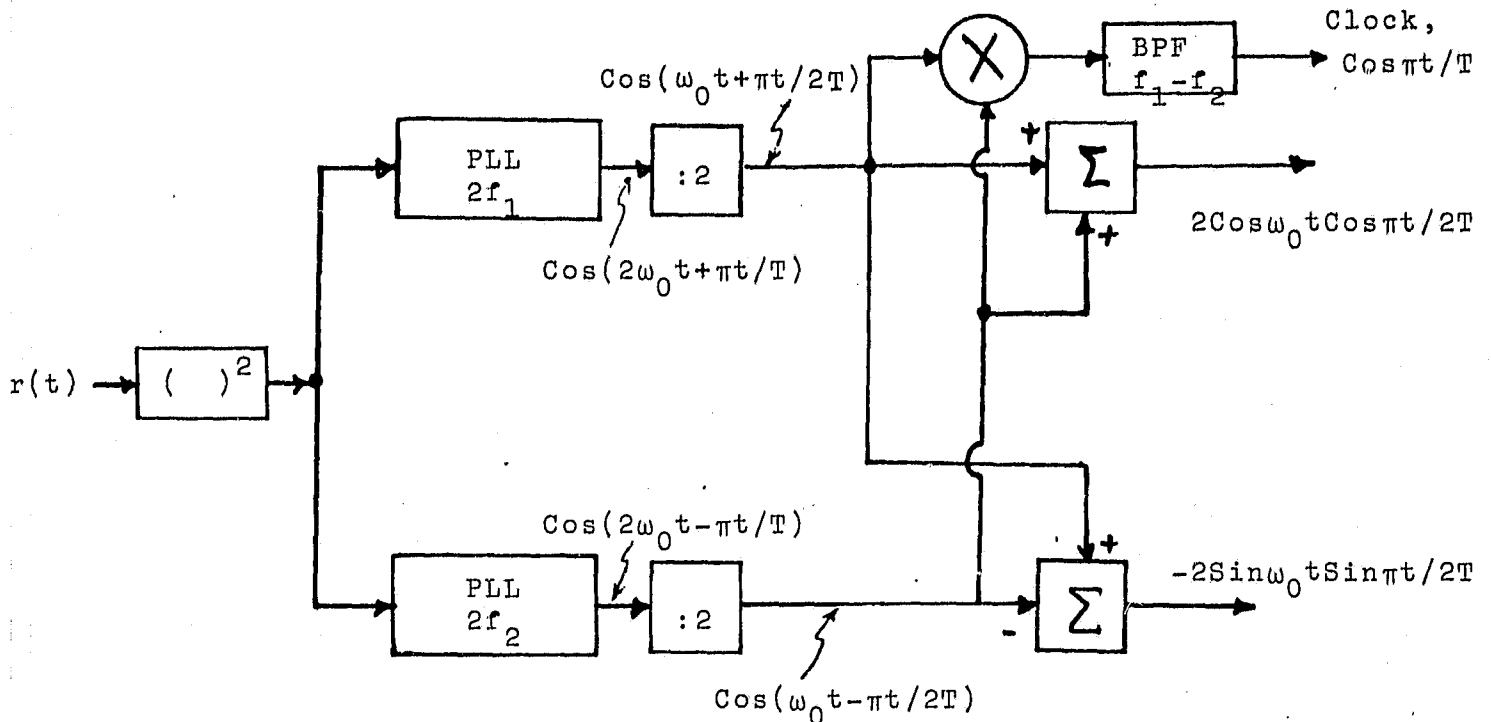


Fig. 13 MSK Receiver Synchronization Circuit

ORIGINAL PAGE IS  
OF POOR QUALITY

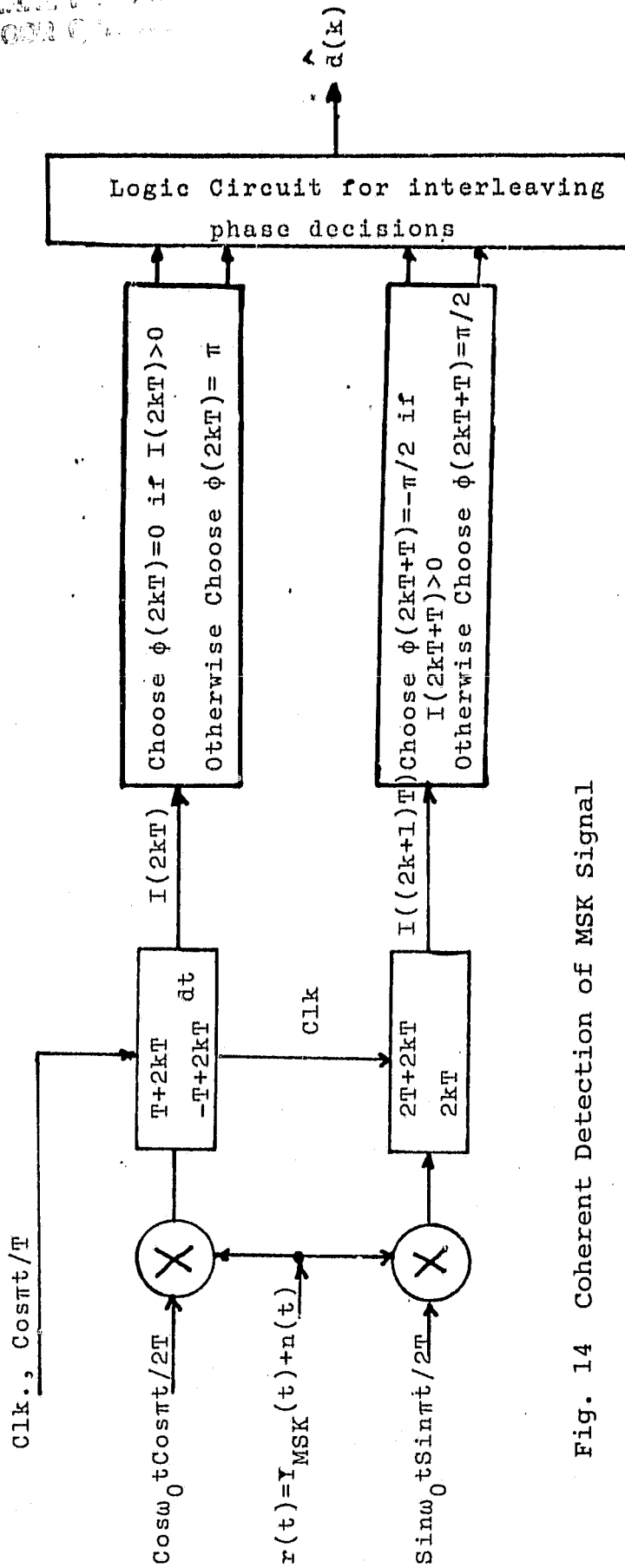


Fig. 14 Coherent Detection of MSK Signal

ORIGINAL PAGE IS  
OF POOR QUALITY

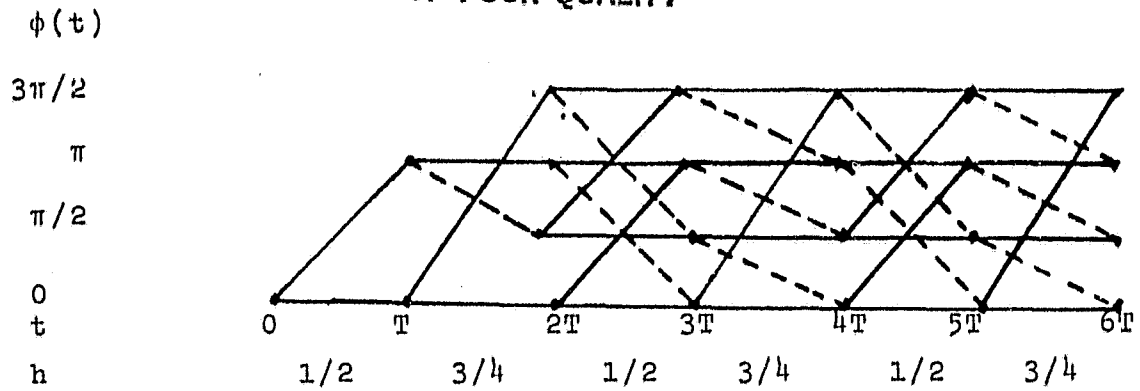


Fig. 15 Phase Versus time Sketched Modulo  $2\pi$  for a phase code with  $h_o = 1/2$  and  $h_e = 3/4$

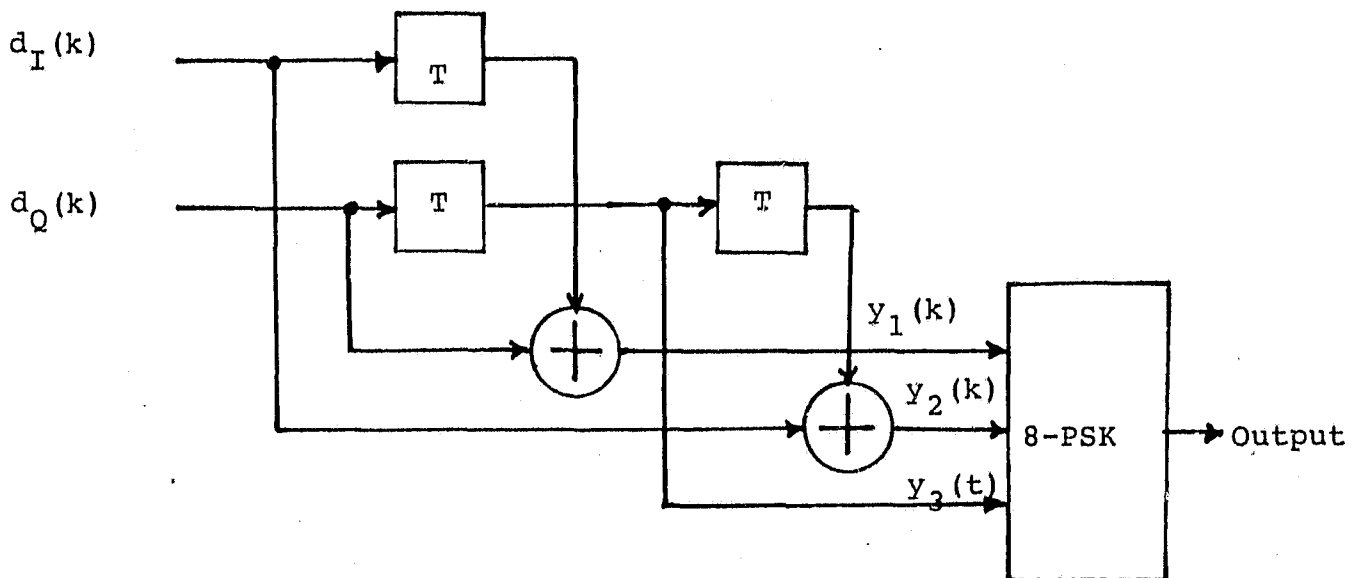


Fig. 16 Realization of 8-PSK Code by Means of a Rate 2/3 Convolutional Code

ORIGINAL PAGE IS  
OF POOR QUALITY

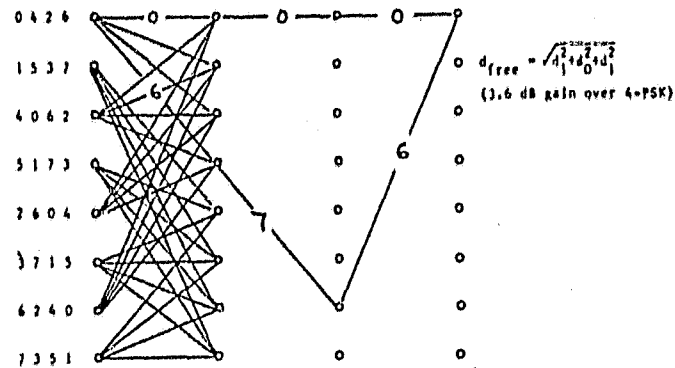


Fig. 17 Periodic trellis structure of rate 2/3 constraint length three convolutional code. The digits on left indicate in top-down fashion the transitions (signals) out of each mode (from Ungerboeck [29]).

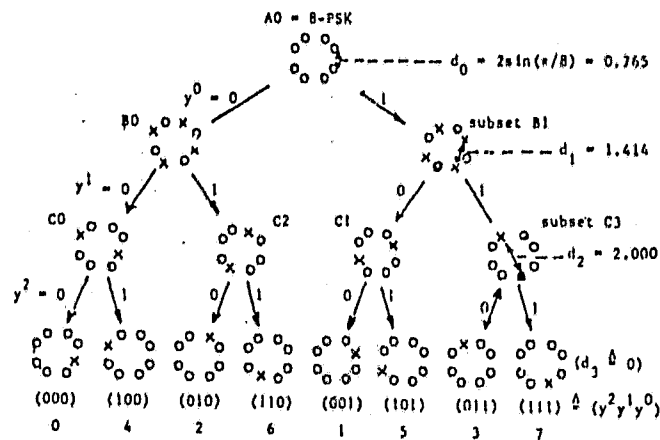


Fig. 18 Illustrations of the partitioning of 8 PSK channel signals into subsets with increasing free subset distance ( $d_0 < d_1 < d_2$ ), so as to achieve mapping by set partitioning (from Ungerboeck [29]).

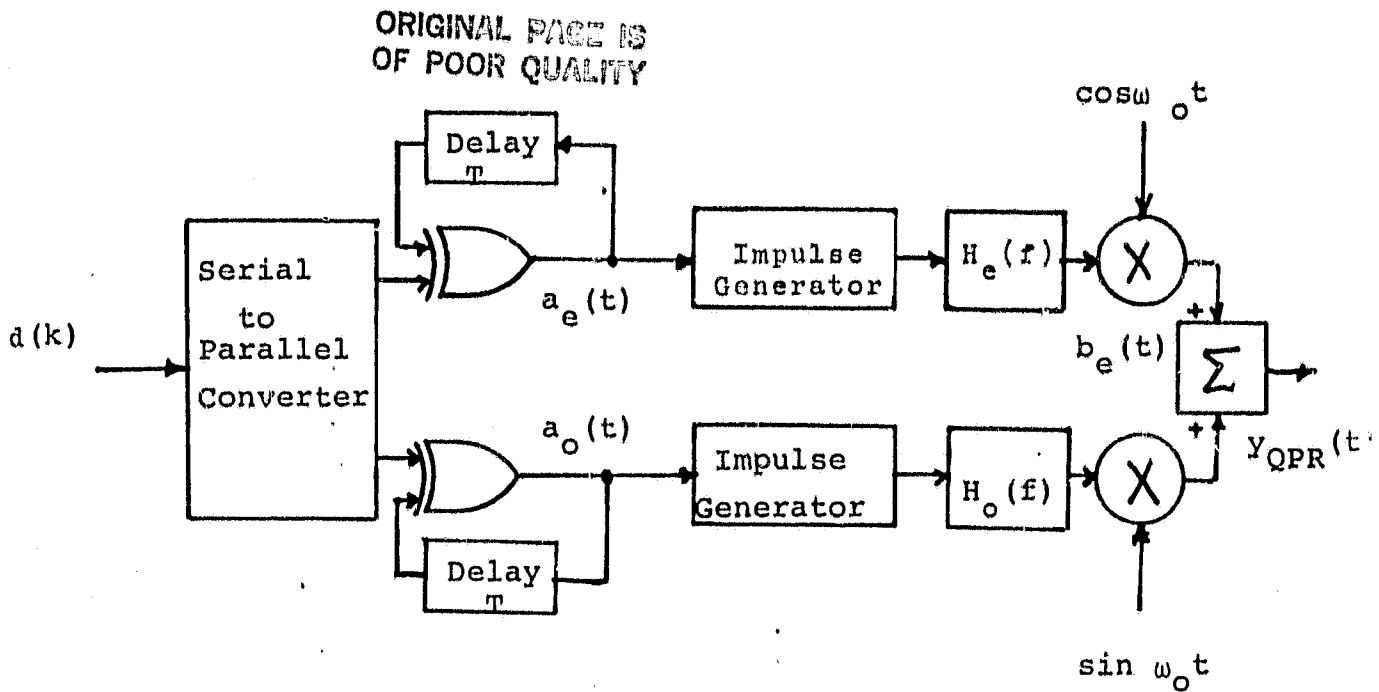


Fig. 19 Block Diagram of a QPR Modulator

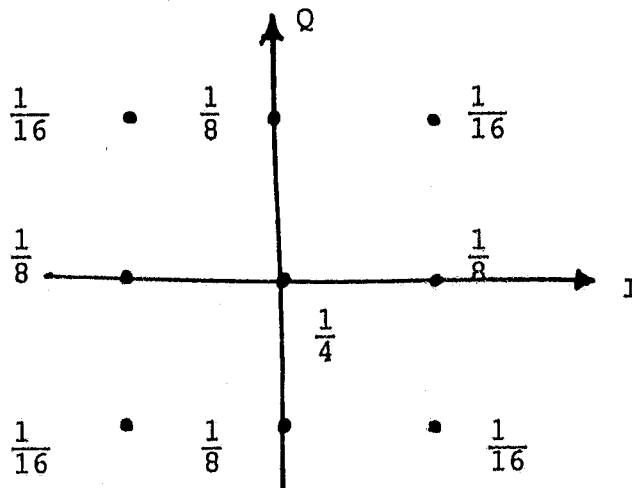


Fig. 20 Signal Constellation of QPR with the Corresponding a Priori Probabilities

ORIGINAL PAGE IS  
OF POOR QUALITY.

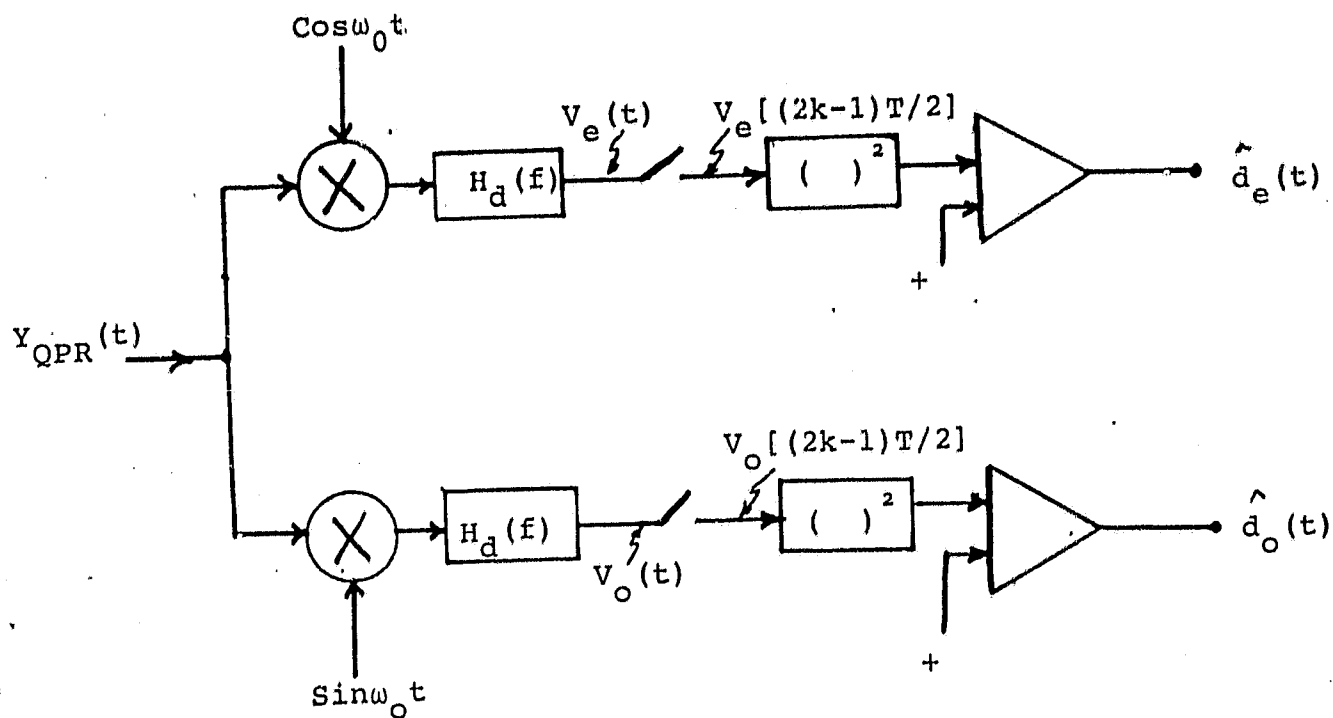


Fig. 21 Block Diagram of a QPR Demodulator

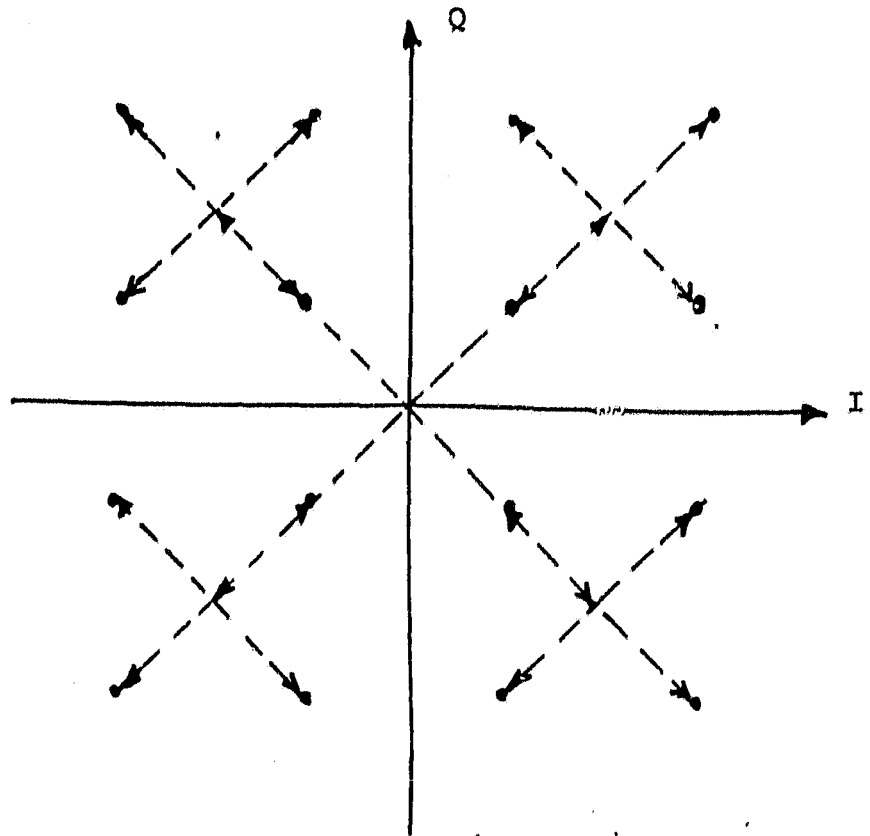


Fig. 22 Signal Constalution of QASK

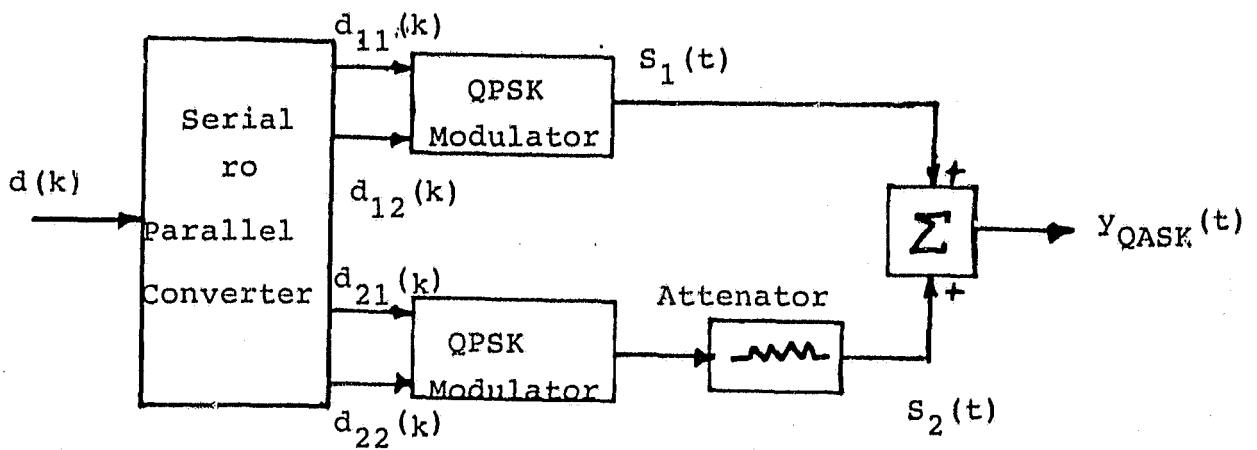


Fig. 23 Superposed QASK Modulator

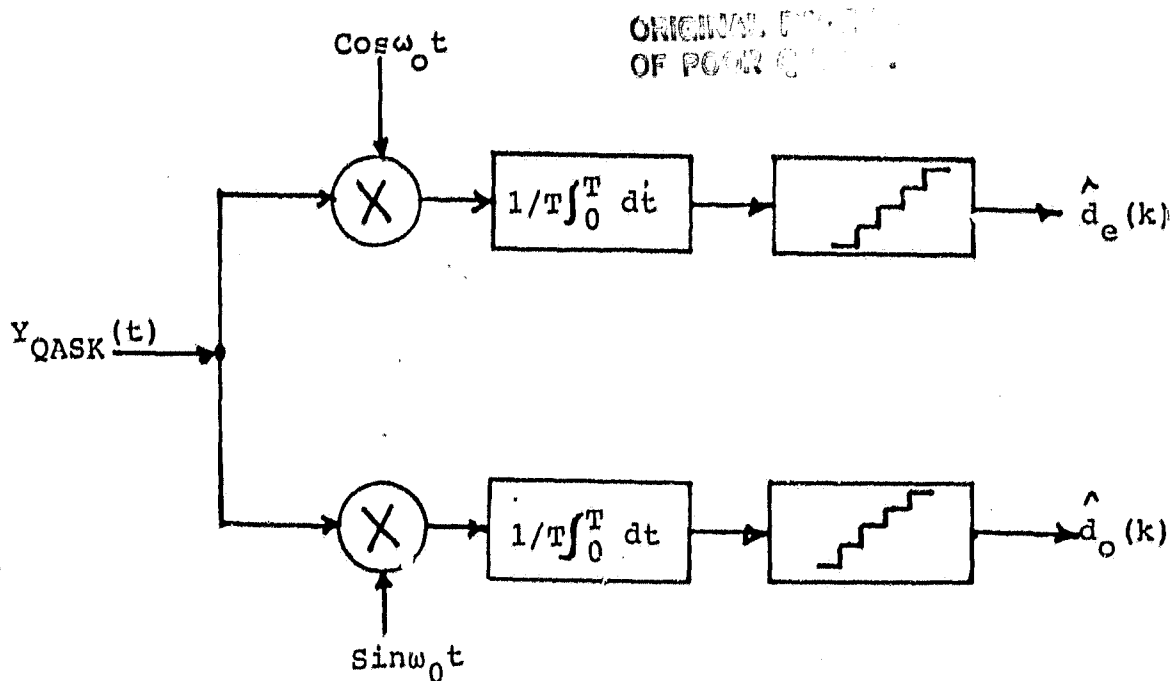


Fig. 24 QASK Demodulator with Perfect Synchronization

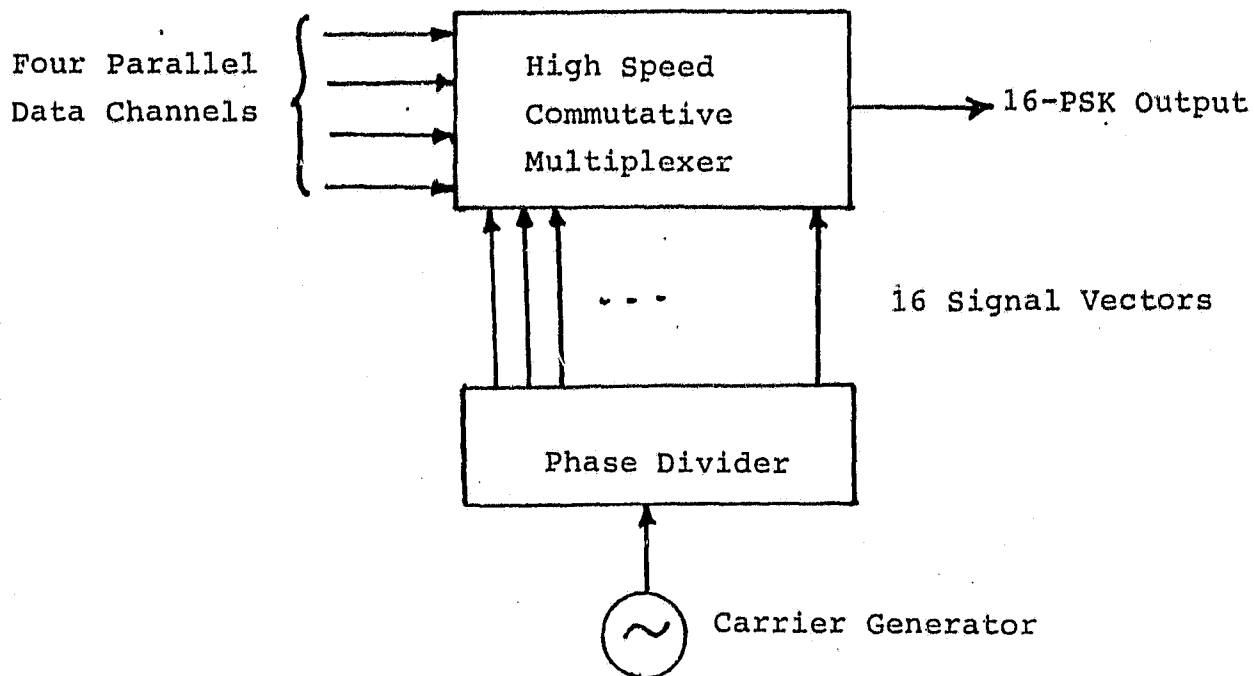


Fig. 25 High Speed 16-PSK Modulator

ORIGINAL PAGE IS  
OF POOR QUALITY

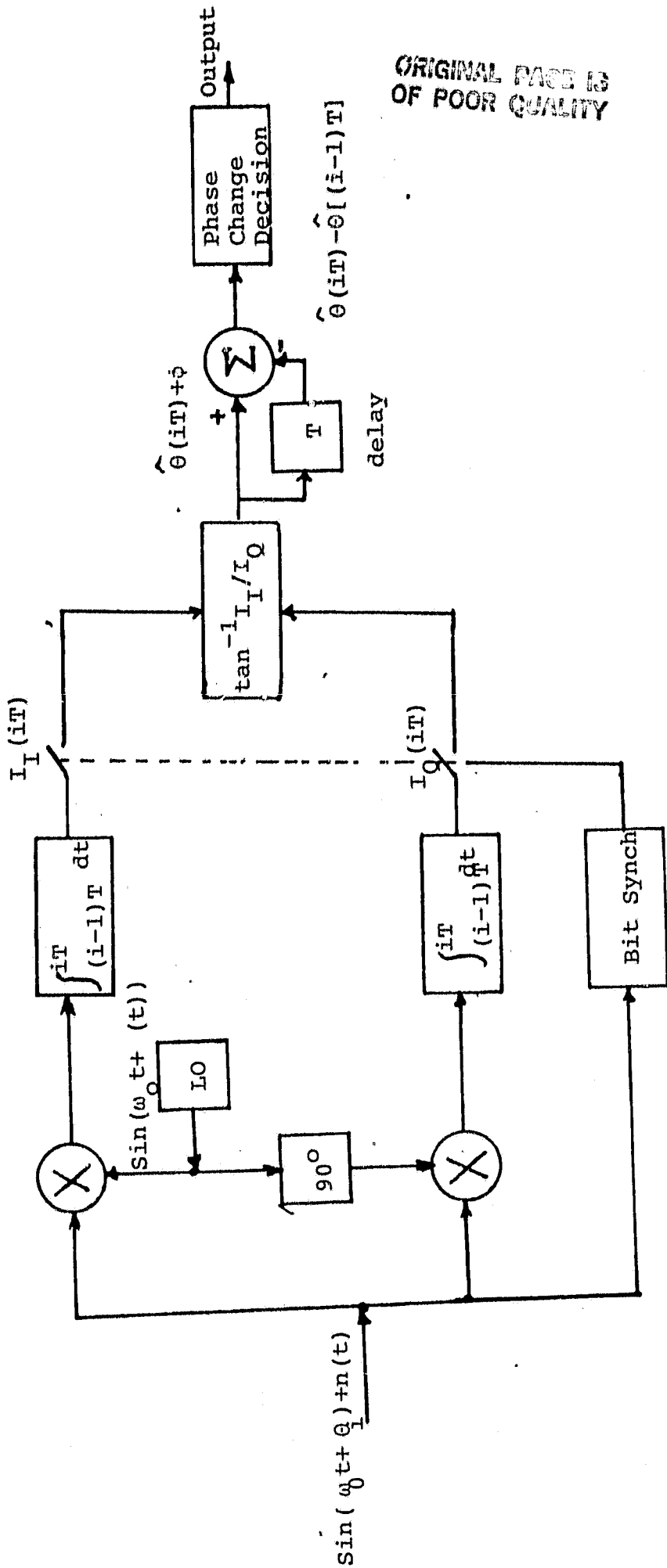


Fig. 26 Block Diagram of a Differentially Coherent Detector for 16-PSK Differentially Encoded.

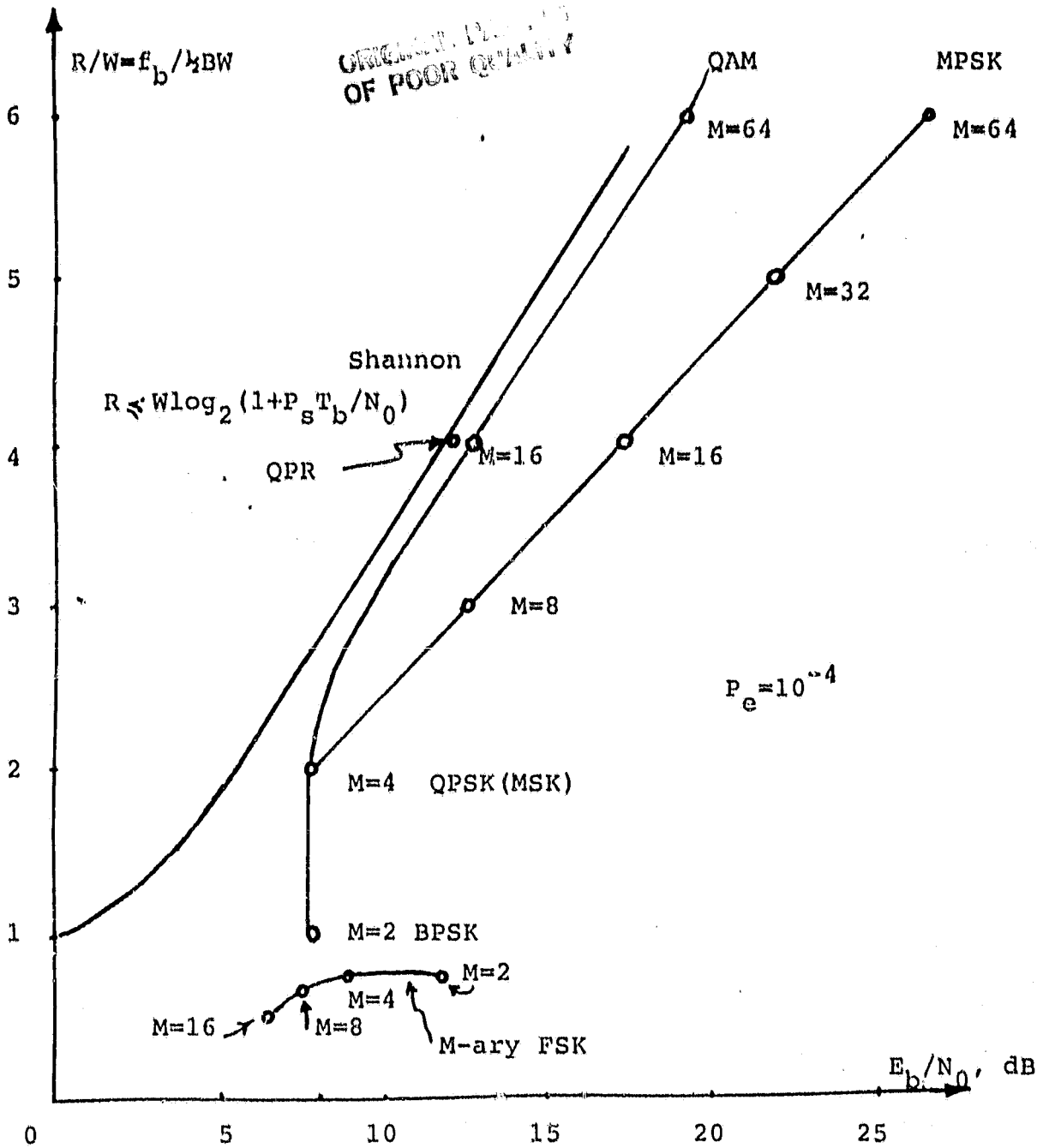


Fig. 27 Comparison of Modulation Techniques

VI. References

- [1] J. D. Oetting, "A Comparison of Modulation Techniques for Digital Radio", IEEE Trans. on Comm, Vol. COM-27, No. 12, Dec. 1979, pp. 1752-1762.
- [2] J. J. Spilker, Jr., Digital Communications by Satellite, Prentice Hall, 1977.
- [3] S. A. Rhodes, "Effect of Hardlimiting on Bandlimited Transmission with Conventional and Offset QPSK Modulation", Proc. Nat. Telecommunications Conf., Houston, Texas 1972, pp. 20F-1-20F-7.
- [4] H. Taub and D. L. Schilling, Principles of Communication Systems, McGraw Hill, 1971.
- [5] S. A. Rhodes, "Performance of Offset QPSK Communications with Partially-Coherent Detection", Proc. Nat. Telecommunications Conf. 1973.
- [6] R. Fang, "Quaternary Transmission Over Satellite Channels with Cascaded Nonlinear Element and Adjacent Channel Interference", IEEE Trans. on Comm, May 1981.
- [7] D. Divesalar and M. K. Simon, "The Power Spectral Density of Digital Modulations Transmitted Over Nonlinear Channels", IEEE Trans. on Comm, Vol. COM-30, No. 1, pp 142-151, Jan 1982.
- [8] R. DeBuda, "Coherent Demodulation of Frequency Shift Keying with Low Deviation Ratio", IEEE Trans. on Comm, Vol. COM-20, pp. 429-435, June 1972.
- [9] H. E. VanDen Elzer and P. VanderWurf, "A Simple Method of Calculating the Characteristics of PSK Signals with Modulation Index, 5", IEEE Trans. Comm, Vol. COM-20, No. 2, April 1972. pp. 139-147.
- [10] S. A. Gronemeyer and A. L. McBride, "MSK and Offset QPSK Modulation", IEEE Trans. on Comm., Vol COM-24, No. 9 Aug. 1976, pp. 809-820.

- [11] D. H. Morais and K. Feher, "Bandwidth Efficiency and Probability of Error Performance of MSK and Offset QPSK Systems", IEEE Trans. on Comm., Vol. COM-27, No. 12, pp. 1794-1801, Dec. 1979.
- [12] C. R. Ryan, A. R. Hambley and D. E. Vogt, "760 Mbit/s Serial MSK Microwave Modem", IEEE Trans. on Comm, Vol., COM-28, No. 5, May 1980.
- [13] R. E. Ziemer, C. R. Ryan and J. H. Stillwell, "Conversion and Matched Filter Approximations for Serial Minimum Shift Keyed Modulation", IEEE Trans. on Comm., Vol. COM-30, No. 3, March 1982.
- [14] F. Amoroso, "Pulse and Spectrum Manipulation in the Minimum (Frequency) Shift Keying (MSK) Format", IEEE Trans. on Comm, pp. 381-384, March 1976.
- [15] M. K. Simon, "A Generalization of Minimum-Shift-Keying (MSK) Type Signalling Based Upon Input Data Symbol Pulse Shaping", IEEE Trans. on Comm., Vol. COM-24, No. 8, Aug. 1976.
- [16] N. Boutin and S. Morissette, "Useful Signalling Waveform and Related Transmit Filter Functions in Bandwidth Limited Channels", IEEE Trans. on Comm., Vol. COM-29, No. 9, Feb. 1981.
- [17] F. Amoroso, "The Use of Quasi-Bandlimited Pulses in MSK Transmission", IEEE Trans. on Comm., Vol. COM-27, No. 10, Oct. 1979.
- [18] H. Suzuki, "Optimum Gaussian Filter for Differential Detection of MSK", IEEE Trans. on Comm, Vol. COM-29, No. 6, June 1981.
- [19] K. Murota and K. Hirade, "GMSK Modulation for Digital Mobile Radio Telephony", IEEE Trans. on Comm, Vol. COM-29, No. 7, July 1981.
- [20] F. deJager and C. B. Dekker, "Tamed Frequency Modulation, a Novel Method to Achieve Spectrum Economy in Digital Transmission", IEEE Trans. on Comm, Vol. COM-26, No. 5, May 1978.

- [21] D. Mulwijk, "Correlative Phase Shift Keying-A Class of Constant Envelope Modulation Techniques", IEEE Trans. on Comm, Vol. COM-29, No. 3, March 1981.
- [22] V. K. Prabhu, "PSK Type Modulation with Overlapping Baseband Pulses", IEEE Trans. on Comm, Vol. COM-25, No. 9 Sept. 1977.
- [23] M. C. Austin and M. V. Chang, "Quadrature Overlapped Raised Cosine Modulation", IEEE Trans. on Comm., Vol. COM-29, No. 3, March 1981.
- [24] I. Sasase, Y. Karada and S. Mori, "Bandwidth Efficient Quadrature Overlapped Modulation", Natl. Tele. Conf. Record, 1982, pp. 6F.2.1-6F.2.5.
- [25] S. Kato and K. Feher, "Cross-Correlated Phase Shift Keying (XPSK) System with Improved Envelope Fluctuation", Nat. Tele. Conf. Record, 1982, pp. 2E.1.1-2E.1.5.
- [26] S. Asakawa and F. Sugiyama, "A Compact Spectrum Constant Envelope Digital Phase Modulation", IEEE Trans. on Vehicular Tech., Vol. VT-30, No. 3, Aug. 1981.
- [27] J. M. Wozencraft and I. M. Jacobs, Principles of Communication Engineering, New York, Wiley, 1965.
- [28] J. B. Anderson and D. P. Taylor, "A Bandwidth Efficient Class of Signal-Space Codes", IEEE Trans. on Information Theory, Vol. IT-24, No. 6, pp. 703-712, May 1978.
- [29] G. Ungerboeck, "Channel Coding with MultiLevel/Phase Signals", IEEE Trans. on Info. Theory, Vol. IT-28, No. 1. pp. 55-67, Jan. 1982.
- [30] N. Rydbeck and C. E. Sundberg, "Recent Results on Spectrally Efficient Constant Envelope Digital Modulation Methods", Proc. ICC 1979, Boston, June 1979.

- [31] IEEE Trans. on Comm., "Special Section on Combined Modulation and Encoding", Vol. COM-29, March 1981.
- [32] S. A. Lebowitz and S. A. Rhodes, "Performance of Coded 8-PSK Signalling for Satellite Communications", ICC Conf. Rec., pp. 47.4-47.4.8, June 1981.
- [33] S. G. Wilson, P. J. Schottler and H. A. Sleeper, "Rate 3/4 16-PSK Phase Codes", Proc. Nat. Tele. Conf. 1982, pp. 6F.1.1-6F.1.5.
- [34] R. Fang, "A Bandwidth and Power Efficient Modulation System", COMSAT Labs. Tech. Rep. No. WP2891/ST1IR2.
- [35] D. P. Taylor and H. C. Chan, "A Simulation Study of Two Bandwidth Efficient Modulation Techniques", IEEE Trans. Comm, Vol. COM-29, No. 3, March 1981.
- [36] K. Feher, Digital Communications Microwave Applications, Ch.7 by A. Lender, Prentice-Hall, N. J. 1981.
- [37] C. W. Anderson and S. G. Barber, "Modulation Considerations for a 91 Mbit/s Digital Radio", IEEE Trans. on Comm, Vol. COM-26, pp. 523-528, May 1978.
- [38] M. K. Simon and J. G. Smith, "Hexagonal Multiple Phase and Amplitude Shift Keyed Signal Sets", IEEE Trans. Comm, Oct. 1973, pp. 1108-1115.
- [39] K. Miyauchi, S. Seki and H. Ishio, "New Technique for Generating and Detecting Multilevel Signal Formats", IEEE Trans. Comm., Vol-COM-24, pp. 263-267, Feb. 1976.
- [40] M. Washio, T. Shimamura, N. Koniyama and Y. Takimoto, "16-Gb/s 16-level Superposed PSK Modem with Baseband Signal Processing Coherent Demodulator", IEEE Trans. on Microwave Theory and Tech, Vol. MTT-26, No. 12, Dec. 1978.

- [41] H. Ishio, et. al., "A New Multilevel Modulation and Demodulation System for Carrier Digital Transmission", ICC 76, pp. 29.7-29.12.
- [42] M. Simon and J. G. Smith, "Carrier Synchronization and Detection of QASK Signals Sets", IEEE Trans. Comm. Vol, COM-22, No. 2, pp. 98-106, Feb. 1974.
- [43] G. Verdote and A. Leclert, "Universal High Bit Rate Modem for Digital Radio Systems", NTC 1982, pp. 3B.1.1-3B.1.4.
- [44] M. Simon, "An MSK Approach to Offset-QASK", IEEE Trans. on Comm., pp. 921-923, Aug. 1976.
- [45] W. J. Weber, P. H. Stanton and J. J. Sumida, "A Bandwidth Compressive Modulation System Using Multi-Amplitude Minimum Shift Keying (MAMSK)", IEEE Trans. on Comm., Vol. COM-26, May 1978.
- [46] W. A. Wood, "Modulation and Filtering Techniques for 3 bits/Hertz Operation in the 6GHz Frequency Band", ICC77, pp. 5.3.97-5.3.101.